PAPER

Gravitational wave signals in an Unruh–DeWitt detector

IOP Publishing Classical and Quantum Gravity
Class. Quantum Grav. **40** (2023) 035007 (25pp) https://doi.org/10.1088/1361-6382/acabf5

Gravitational wave signals in an Unruh–DeWitt detector

Tomislav Prokopec

Institute for Theoretical Physics, Spinoza Institute & EMME Utrecht University, Princetonplein 5, 3584 CC Utrecht, The Netherlands

E-mail: T.Prokopec@uu.nl

Received 13 July 2022; revised 7 October 2022
Accepted for publication 15 December 2022
Published 13 January 2023

Abstract

We firstly generalize the massive scalar propagator for planar gravitational waves propagating on Minkowski space obtained recently in van Haasteren and Prokopec (2022 arXiv:2204.12930 [gr-qc]). We then use this propagator to study the response of a freely falling Unruh–DeWitt detector to a gravitational wave background. We find that a freely falling detector completely cancels the effect of the deformation of the invariant distance induced by the gravitational waves, such that the only effect comes from an increased average size of scalar field vacuum fluctuations, the origin of which can be traced back to the change of the surface in which the gravitational waves fluctuate. The effect originates from the quantum interference between propagation on off-shell detector's trajectories which probe different spatial gravitational potential induced by the gravitational backreaction from gravitational waves, and it is therefore purely quantum. When resummed over classical graviton insertions, gravitational waves generate cuts on the imaginary axis of the complex $\Delta\tau$-plane (where $\Delta\tau = \tau - \tau'$ denotes the difference of proper times), and the discontinuity across these cuts is responsible for a continuum of energy transitions induced in the Unruh–DeWitt detector. Not surprisingly, we find that the detector's transition rate is exponentially suppressed with increasing energy and the mass of the scalar field. What is surprising, however, is that the transition rate is a *non-analytic function* of the gravitational field strain. This means that, no matter how small is the gravitational field amplitude, expanding in powers of the gravitational field strain cannot approximate well the detector's transition rate. We present numerical and approximate analytical results for the detector's

transition rate both for circularly polarized and for polarized monochromatic, unidirectional, gravitational waves.

Keywords: Unruh–DeWitt detector, gravitational waves,
quantum field theory in curved spaces

(Some figures may appear in colour only in the online journal)

1. Introduction

In this work we calculate the response of a freely falling Unruh–DeWitt detector which couples to a massless or massive scalar field fluctuating in the presence of planar gravitational waves propagating on Minkowski spacetime. This work builds on earlier studies [1–9], which address some aspects of the problem of how planar gravitational waves affect scalar fields. In particular the authors of [9] investigate the response of freely-falling and accelerating Unruh–DeWitt detectors [10–12] in the presence of gravitational waves. In this work we generalize their analysis by using the propagator recently obtained in [1]. For simplicity, we do not analyze here the response of the detector moving along noninertial trajectories.

1.1. The model

In this work we consider a real, self-interacting scalar field $\phi(x)$ whose action and Lagrangian are,

$$S[\phi]=\int \mathrm{d}^D x\sqrt{-g}\,\mathcal{L}_\phi,\qquad \mathcal{L}_\phi=-\frac{1}{2}(\partial_\mu\phi)(\partial_\nu\phi)g^{\mu\nu}-\frac{m^2}{2}\phi^2-\frac{\lambda}{4!}\phi^4, \quad (1.1)$$

where $g=\det[g_{\mu\nu}]$, $g^{\mu\nu}$ is the inverse of the metric tensor $g_{\mu\nu}$, m is the field's mass and λ is the self-interaction coupling strength. We work in natural units in which $c=1$, but keep the dependence on $\hbar$ explicit. This means that the dimension of the field ϕ and the mass m is m^{-1}, and λ is dimensionless. To restore the physical dimension of m, one ought to rescale it as, $m\to mc/\hbar$.

1.1.1. Gravitational waves. We are interested in understanding the effects of gravitational waves on scalar fields. A convenient representation for a gravitational wave background is,

$$g_{\mu\nu}(x)=\eta_{\mu\nu}+h_{\mu\nu}(x), \quad (1.2)$$

where $h_{\mu\nu}(x)$ is a perturbation of the metric tensor $g_{\mu\nu}$ around flat Minkowski space, characterized by Minkowski metric $\eta_{\mu\nu}$, which is in Cartesian coordinates a $D\times D$ diagonal matrix of the form, $\eta_{\mu\nu}=\mathrm{diag}(-1,1,1,\dots)$. In the traceless-transverse gauge (in which the gravitational field perturbation $h_{\mu\nu}$ is gauge invariant to linear order in the gravitational field), planar gravitational waves moving in the x^{D-1} direction ($x^{D-1}\to z$ when $D=4$) satisfy $h_{0\mu}=0$ and

$$h_{ij}(u)=\begin{pmatrix} h_{xx}(u) & h_{xy}(u) & \cdots & h_{xD-2}(u) & 0\\ h_{xy}(u) & h_{yy}(u) & \cdots & h_{yD-2}(u) & 0\\ \vdots & \vdots & \vdots & \cdots & \vdots\\ h_{xD-2}(u) & h_{yD-2}(u) & \cdots & h_{D-2D-2}(u) & 0\\ 0 & 0 & \cdots & 0 & 0\end{pmatrix}, \quad (1.3)$$

where $u = t - x^{D-1}$ is a lightcone coordinate. Note that some of the elements of h_{ij} in equation (1.3) may vanish. In $D = 4$ dimensions this simplifies to planar gravitational waves with nonvanishing elements in the $xy-$plane. In practical calculations it is often convenient to simplify (1.3) by assuming that nonvanishing elements of h_{ij} are in the upper left 2×2 block.

In this work we generalize the monochromatic wave background considered in [1] to the case when the gravitational wave strain, $h_{ij} = h_{ij}(u)$, is characterized by a general function of u propagating in the x^{D-1} direction. Motivated by the form of gravitational waves emitted by realistic sources, whose wave form can be decomposed into the fundamental mode of frequency ω_g, and the higher overtones (whose frequencies are $n\omega_g$), we shall consider gravitational waves of the form,

$$h_{ij}(u) = \sum_{n=1}^{\infty} h_{ij}^{(n)} \cos\left(n\omega_g u + \psi_{ij}^{(n)}\right), \tag{1.4}$$

where $h_{ij}^{(n)}$ and $\psi_{ij}^{(n)}$ are the (time independent) gravitational field amplitudes and phases of the n-th harmonic. Such elliptically polarized gravitational waves are formed by binary systems whose components harbor angular momentum and/or strong magnetic fields [13, 14]. It is important to keep in mind that, even when gravitational waves are emitted as circularly polarized, the perceived amplitudes of the $+$ and $\times$ polarizations will differ, unless the source is *face on*, i.e. the inclination angle is zero. This means that the only fixed characteristic of observed gravitational waves is the relative phase difference, $\Delta\psi = \psi_+ - \psi_\times = \pm\pi/2$.

The gravitational waves considered here have a phase velocity, $\vec{v}_{\rm ph} = \hat{z}$, and are often referred to as the positive frequency solutions. In addition there are negative frequency gravitational waves, with an opposite phase velocity ($\vec{v}_{\rm ph} = -\hat{z}$), for which $h_{ij} = h_{ij}(v)$, with $v = t + z$ ($v = t + x^{D-1}$ in the D dimensional case). Sufficiently close to the gravitational wave source the gravitational wave propagates radially, such that in a relatively small spatial volume one can approximate the wave by $h_{ij}(u)$.

2. Scalar propagator

Variation of the action (1.1) gives a Klein–Gordon equation satisfied by the scalar field operator $\hat{\phi}(x)$,

$$\left(\Box - m^2\right)\hat{\phi}(x) = 0, \tag{2.1}$$

where $\Box = \frac{1}{\sqrt{-g}}\partial_\mu\sqrt{-g}g^{\mu\nu}\partial_\nu$ is the d'Alembertian operator as it acts on a scalar field, and we have neglected in equation (2.1) the quartic self-coupling. The positive and negative frequency Wightman functions are defined as the following two-point functions,

$$i\Delta^{(+)}(x;x') = \langle\Omega|\,\hat{\phi}(x)\hat{\phi}(x')\,|\Omega\rangle\,, \tag{2.2}$$

$$i\Delta^{(-)}(x;x') = \langle\Omega|\,\hat{\phi}(x')\hat{\phi}(x)\,|\Omega\rangle\,, \tag{2.3}$$

where $|\Omega\rangle$ denotes a state of the scalar field, which for simplicity we choose to be the vacuum state. When the field operator in equation (2.1) is expanded in terms of the momentum space mode functions, one can reduce the problem of obtaining the Wightman functions to performing the momentum integrals in equations (A.2) and (A.3) over products of the mode functions. These integrals can be performed by a straightforward generalization of the method used in [1], whose the main steps outline in appendix A. From equations (A.14)–(A.17) it immediately follows,

$$i\Delta^{(\pm)}(x;x') = \frac{\hbar m^{D-2}}{(2\pi)^{\frac{D}{2}}[\gamma(u)\gamma(u')]^{\frac{1}{4}}\sqrt{\det[\mathcal{G}^{ij}](u;u')}}\frac{K_{\frac{D-2}{2}}\left(m\sqrt{\Delta\bar{x}^2_{(\pm)}}\right)}{\left(m\sqrt{\Delta\bar{x}^2_{(\pm)}}\right)^{\frac{D-2}{2}}}, \quad (2.4)$$

where $K_\nu(z)$ denotes the modified Bessel function of the second kind, and $\Delta\bar{x}^2_{(\pm)}(x;x')$ are the deformed distance functions, which in lightcone coordinates can be written as,

$$\Delta\bar{x}^2_{(\pm)}(x;x') = -(\Delta u\mp i\epsilon)(\Delta v\mp i\epsilon) + \begin{pmatrix}\Delta x & \Delta y & \cdots & \Delta x^{D-2}\end{pmatrix}\cdot\mathcal{G}(u;u')\cdot\begin{pmatrix}\Delta x\\ \Delta y\\ \vdots\\ \Delta x^{D-2}\end{pmatrix}, \quad (2.5)$$

and in Cartesian coordinates,

$$\Delta\bar{x}^2_{(\pm)}(x;x') = -(\Delta t\mp i\epsilon)^2 + \begin{pmatrix}\Delta x & \Delta y & \cdots & \Delta x^{D-2}\end{pmatrix}\cdot\mathcal{G}(u;u')\cdot\begin{pmatrix}\Delta x\\ \Delta y\\ \vdots\\ \Delta x^{D-2}\end{pmatrix} + \Delta x^2_{D-1}, \quad (2.6)$$

where $\Delta x^\mu = x^\mu - x'^\mu$, where the deformation matrix $\mathcal{G}_{ij}(u;u')$ is given by,

$$\mathcal{G}_{ij}(u;u') = \begin{pmatrix}\mathcal{G}_{xx}(u;u') & \mathcal{G}_{xy}(u;u') & \cdots & \mathcal{G}_{xD-2}(u;u')\\ \mathcal{G}_{xy}(u;u') & \mathcal{G}_{yy}(u;u') & \cdots & \mathcal{G}_{yD-2}(u;u')\\ \vdots & \vdots & \vdots & \vdots\\ \mathcal{G}_{xD-2}(u;u') & \mathcal{G}_{yD-2}(u;u') & \cdots & \mathcal{G}_{yD-2}(u;u')\end{pmatrix}. \quad (2.7)$$

Note that $\mathcal{G}_{ij}(u;u')$ is the inverse of the corresponding momentum space deformation matrix $\mathcal{G}^{ij}(u;u')$, $\mathcal{G}^{ik}(u;u')\mathcal{G}_{kj}(u;u') = \delta^i_j$. The general form of $\mathcal{G}^{ij}(u;u')$ is,

$$\mathcal{G}^{ij}(u;u')(u;u') = \frac{1}{\Delta u}\int_{u'}^{u}\begin{pmatrix}g^{xx}(\bar{u}) & g^{xy}(\bar{u}) & \cdots & g^{xD-2}(\bar{u})\\ g^{xy}(\bar{u}) & g^{yy}(\bar{u}) & \cdots & g^{yD-2}(\bar{u})\\ \vdots & \vdots & \vdots & \vdots\\ g^{xD-2}(\bar{u}) & g^{yD-2}(\bar{u}) & \cdots & g^{D-2D-2}(\bar{u})\end{pmatrix}\mathrm{d}\bar{u}, \quad (2.8)$$

where $g^{ij}(u)$ denote the inverse of $g_{ij}(u)$. For example, for gravitational waves oscillating in the xy plane, only the distances in this plane (which we denote by $\perp$) get deformed, such that the nontrivial elements of the deformation matrix are,

$$\begin{aligned}\mathcal{G}^{ij}_\perp(u;u') &= \frac{1}{\Delta u}\int_{u'}^{u}\begin{pmatrix}g^{xx}(\bar{u}) & g^{xy}(\bar{u})\\ g^{xy}(\bar{u}) & g^{yy}(\bar{u})\end{pmatrix}\mathrm{d}\bar{u}\\ &= \frac{1}{\Delta u}\int_{u'}^{u}\frac{1}{\gamma(u)}\begin{pmatrix}g_{yy}(\bar{u}) & -g_{xy}(\bar{u})\\ -g_{xy}(\bar{u}) & g_{xx}(\bar{u})\end{pmatrix}\mathrm{d}\bar{u}, \end{aligned} \quad (2.9)$$

where $\gamma(u) = \det[g_{ij}(u)]$. For monochromatic, circularly polarized gravitational waves in linear representation one obtains (see section 3 of [1]),

$$\mathcal{G}^\perp_{ij}(u;u') = \frac{1}{\gamma\det[\mathcal{G}^{ij}_\perp](u;u')}\begin{pmatrix}1+h\frac{\sin(\omega_g u)-\sin(\omega_g u')}{\omega_g\Delta u} & -h\frac{\cos(\omega_g u)-\cos(\omega_g u')}{\omega_g\Delta u}\\ -h\frac{\cos(\omega_g u)-\cos(\omega_g u')}{\omega_g\Delta u} & 1-h\frac{\sin(\omega_g u)-\sin(\omega_g u')}{\omega_g\Delta u}\end{pmatrix}, \quad (2.10)$$

$$\det\Big[\mathcal{G}^{ij}_{\perp}(u;u')\Big]=\frac{1}{\gamma^2}\bigg[1-h^2j_0^2\bigg(\frac{\omega_g\Delta u}{2}\bigg)\bigg], \tag{2.11}$$

where $j_0(z)=\sin(z)/z$ is the spherical Bessel function, $\gamma(u)=\det[g_{ij}(u)]=1-h^2$ is time independent, $h=h_+=h_\times$, and $h_+=h_{xx}=-h_{yy}$ and $h_\times=h_{xy}$ are the amplitudes of the two polarizations. The matrix $\mathcal{G}^{\perp}_{ij}(u;u')$ deforms distances in position space according to equations (2.5) and (2.6).

On the other hand, for singly polarized monochromatic waves fluctuating in the xy-plane one obtains for the $(+)$-polarized waves ($h_+\neq 0$, $h_\times=0$),

$$\mathcal{G}^{ij}_{\perp}=\frac{2}{\omega_g\Delta u}\frac{1}{\sqrt{1-h_+^2}} \times\left\{\begin{pmatrix}\arctan\Big[\sqrt{\frac{1-h_+}{1+h_+}}\tan\Big(\frac{\omega_g u}{2}\Big)\Big] & 0\\ 0 & \arctan\Big[\sqrt{\frac{1+h_+}{1-h_+}}\tan\Big(\frac{\omega_g u}{2}\Big)\Big]\end{pmatrix}-(u\to u')\right\}, \tag{2.12}$$

and for the $(\times)$-polarized waves ($h_+=0$, $h_\times\neq 0$),

$$\mathcal{G}^{ij}_{\perp}=\frac{1}{\omega_g\Delta u}\frac{1}{\sqrt{1-h_\times^2}} \times\left\{\begin{pmatrix}\arctan\Big[\frac{1}{\sqrt{1-h_\times^2}}\tan(\omega_g u)\Big] & -\arctan\Big[\frac{h_\times}{\sqrt{1-h_\times^2}}\sin(\omega_g u)\Big]\\ -\arctan\Big[\frac{h_\times}{\sqrt{1-h_\times^2}}\sin(\omega_g u)\Big] & \arctan\Big[\frac{1}{\sqrt{1-h_\times^2}}\tan(\omega_g u)\Big]\end{pmatrix}-(u\to u')\right\}, \tag{2.13}$$

respectively.

From the Wightman functions (2.4) one can easily construct the Feynman propagator. In lightcone coordinates we have,

$$\begin{aligned} i\Delta_{\rm F,LC}(x;x')&\equiv\Theta(\Delta u)i\Delta^{(+)}(x;x')+\Theta(-\Delta u)i\Delta^{(-)}(x;x')\\ &=\frac{\hbar m^{D-2}}{(2\pi)^{\frac{D}{2}}[\gamma(u)\gamma(u')]^{\frac{1}{4}}\sqrt{\det[\mathcal{G}^{ij}](u;u')}}\frac{K_{\frac{D-2}{2}}\Big(m\sqrt{\Delta\bar{x}^2_{\rm F,LC}}\Big)}{\Big(m\sqrt{\Delta\bar{x}^2_{\rm F,LC}}\Big)^{\frac{D-2}{2}}}, \end{aligned} \tag{2.14}$$

and in Cartesian coordinates,

$$\begin{aligned} i\Delta_{\rm F}(x;x')&\equiv\Theta(\Delta t)i\Delta^{(+)}(x;x')+\Theta(-\Delta t)i\Delta^{(-)}(x;x')\\ &=\frac{\hbar m^{D-2}}{(2\pi)^{\frac{D}{2}}[\gamma(u)\gamma(u')]^{\frac{1}{4}}\sqrt{\det[\mathcal{G}^{ij}](u;u')}}\frac{K_{\frac{D-2}{2}}\Big(m\sqrt{\Delta\bar{x}^2_{\rm F}}\Big)}{\Big(m\sqrt{\Delta\bar{x}^2_{\rm F}}\Big)^{\frac{D-2}{2}}}. \end{aligned} \tag{2.15}$$

Both propagators (2.14) and (2.15) are suitable for perturbative studies, the former for the initial value problem defined on an $u=$ constant hypersurface, the latter on a $t=$ constant hypersurface. However, the two $i\epsilon$ prescriptions differ,

$$\Delta\bar{x}^2_{\rm F,LC}(x;x')=-(|\Delta u|-i\epsilon)(\pm\Delta v-i\epsilon)+\|\Delta\vec{x}_\perp\|^2,\ \ \Delta\bar{x}^2_{\rm F}(x;x')=-(|\Delta t|-i\epsilon)^2+\|\Delta\vec{x}\|^2. \tag{2.16}$$

That means that the imaginary parts of the propagators differ. Both prescriptions are legitimate, as they are designated to study inequivalent perturbative evolution problems.

From equations (2.14) and (2.15) one easily obtains the corresponding Dyson propagators,

$$i\Delta_{\rm D,LC}(x;x') = \big[i\Delta_{\rm F,LC}(x;x')\big]^*, \qquad i\Delta_{\rm D}(x;x') = \big[i\Delta_{\rm F}(x;x')\big]^*, \tag{2.17}$$

which are important for studying time evolution of Hermitian operators in interacting quantum field theories.

2.1. One-loop results

In what follows we briefly summarize the one-loop calculations from [1] for the generalized gravitational waves of the form (1.3).

For the one-loop effective action calculation and one-loop scalar mass induced by the scalar self-interaction, one needs the coincident propagator (2.14) and (2.15), which is of the same form as in equation (4.4) of [1],

$$i\Delta_{\rm F}(x;x) = \frac{\hbar m^{D-2}}{(4\pi)^{D/2}\sqrt{\gamma(u)\det[\mathcal{G}^{ij}(u;u)]}}\Gamma\Big(1-\frac{D}{2}\Big), \tag{2.18}$$

where $\gamma(u) = \det[g_{ij}]$ and $\det[\mathcal{G}^{ij}(u;u)]$ is the determinant of the $\mathcal{G}^{ij}(u;u)$ matrix in equation (2.8) evaluated at spacetime coincidence. Applying the l'Hospital rule to equation (2.9) yields,

$$\mathcal{G}^{ij}(u;u) = \begin{pmatrix} g^{xx}(u) & g^{xy}(u) & \cdots & g^{xD-2}(u) \\ g^{xy}(u) & g^{yy}(\bar{u}) & \cdots & g^{yD-2}(u) \\ \vdots & \vdots & \vdots & \vdots \\ g^{xD-2}(u) & g^{xD-2}(u) & \cdots & g^{D-2D-2}(u) \end{pmatrix} \equiv g^{ij}(u), \tag{2.19}$$

from which it immediately follows that, $\det[\mathcal{G}^{ij}](u;u) = \det[g^{ij}(u)] = 1/\gamma(u)$, and therefore,

$$\gamma(u)\det[\mathcal{G}^{ij}(u;u)] = 1\,. \tag{2.20}$$

This shows that both, the one-loop effective action and the one-loop scalar mass reduce to those of Minkowski space in equations (4.12) and (4.15) of [1].

The calculation of the one-loop energy momentum tensor is more involved, but the procedure is the same as for the polarized gravitational waves in linear representation in appendix A of [1], and the resulting renormalized energy momentum tensor is identical in form as in equations ((5.29) and (5.30)) of [1],

$$\begin{aligned}\langle\Omega|T^*[\hat{T}^{\rm ren}_{\mu\nu}(x)]|\Omega\rangle = &-\frac{\hbar m^4}{64\pi^2}\left[\ln\left(\frac{m^2}{4\pi\mu^2}\right)+\gamma_E-\frac{3}{2}\right]g_{\mu\nu}(u) - \frac{\hbar m^2}{96\pi^2} \\ &\times\left[\log\left(\frac{m^2}{4\pi\mu^2}\right)+\gamma_E-1\right]G_{\mu\nu}(u),\end{aligned} \tag{2.21}$$

where $G_{\mu\nu}(u)$ is the classical Einstein tensor associated with the metric in equations (1.2) and (1.3). The counterterms needed to renormalize (2.21) are generated by the cosmological constant action and the Hilbert–Einstein action, as detailed in [1]. Upon recalling that gravitational waves carry a classical (Lifshitz) energy-momentum tensor, $T^{\rm class}_{\mu\nu} = -G_{\mu\nu}(u)/(8\pi G)$, the result in equation (2.21) can be intuitively understood as the one-loop scalar matter energy momentum tensor induced by the leading quantum response of the massive scalar field to passing gravitational waves. The result (2.21) cannot be directly compared with that of [15],

where the author considered the one-loop energy-momentum tensor of a massive scalar field observed in a distant future (in which the vacuum state reduces to that of Minkowski space) and argued that the one-loop energy momentum tensor is identical to that in Minkowski vacuum. Note also that, if the gravitational wave amplitude is adiabatically switched off, the result in equation (2.21) reduces to the trivial (Minkowski vacuum) result of [15].

3. Unruh–DeWitt detector

In this section we study the response of a freely falling Unruh–DeWitt detector [10–12] moving in the background of gravitational waves which propagate in the z-direction. This work generalizes the analysis of [9].

3.1. Freely falling observers

The line element for the problem at hand can be written from equation (1.2) as,

$$ds^2 = -dt^2 + dx^i g_{ij}(u) dx^j = -du dv + dx^i g^{\perp}_{ij}(u) dx^j, \tag{3.1}$$

where $g^{\perp}_{ij}(u)$ is a $(D-2)\times(D-2)$ dimensional symmetric metric tensor (in $D=4$ it reduces to a 2×2 dimensional symmetric metric). Useful killing vectors are, $K_v = \partial_v$ and $K_i = \partial_i$ ($i = 1,2,\cdots,D-2$), from which one obtains the corresponding conserved momenta[1],

$$P_v = -(K_v)_\mu \frac{dx^\mu}{d\tau} = \frac{1}{2}\frac{du}{d\tau}, \quad P_i = (K_i)_j \frac{dx^j}{d\tau} = g^{\perp}_{ij}(u)\frac{dx^j}{d\tau}, \quad (i,j = 1,2,\cdots,D-2), \tag{3.2}$$

where (for a later convenience) we chose the geodesic time $\lambda = \tau$ to be the proper time τ, defined by $d\tau^2 = -ds^2$. Upon inserting these equations into the line element (3.1) and dividing by $-d\tau^2$ one obtains,

$$1 = \frac{du}{d\tau}\frac{dv}{d\tau} - \frac{dx^i}{d\tau} g^{\perp}_{ij}(u)\frac{dx^j}{d\tau} = 2P_v\frac{dv}{d\tau} - P_i g^{ij}_{\perp}(u) P_j\,. \tag{3.3}$$

This generates the geodesic equation for $dv/d\tau$,

$$\frac{dv}{d\tau} = \frac{1}{2P_v}\left(1 + P_i g^{ij}_{\perp}(u) P_j\right), \tag{3.4}$$

whose formal solution is,

$$v(\tau) = v_0 + \frac{1}{2P_v}\left(\tau + \frac{P_i}{2P_v}\int_{u_0}^{u} d\bar{u}\, g^{ij}_{\perp}(\bar{u}) P_j\right), \qquad (v_0 \equiv v(0),\ u_0 \equiv u(0)), \tag{3.5}$$

where we made use of, $du/d\tau = 2P_v$. Next, one can solve equation (3.2) to obtain,

$$u(\tau) = u_0 + 2P_v\tau, \qquad (u_0 \equiv u(0)) \tag{3.6}$$

$$x^i(\tau) = x^i_0 + \frac{1}{2P_v}\int_{u_0}^{u} d\bar{u}\, g^{ij}_{\perp}(\bar{u}) P_j, \qquad (x^i_0 \equiv x^i(0)), \tag{3.7}$$

such that equation (3.5) can be also written as,

$$v(\tau) = v_0 + \frac{1}{2P_v}\left(\tau + P_i(x^i(u) - x^i_0)\right). \tag{3.8}$$

[1] Recall that each Killing vector K obeys a Killing equation, $\nabla_{(\mu}K_{\nu)} = 0$, and generates a conserved quantity, $P = K_\mu \frac{dx^\mu}{d\lambda}$.

From equation (3.6) we see that one can always replace τ with u,

$$\tau(u) = \frac{u-u_0}{2P_v}. \tag{3.9}$$

3.2. Unruh–DeWitt detector

An Unruh–DeWitt detector [10–12] is a detector with a monopolar coupling to a scalar field ϕ, which can be represented by the interaction Lagrangian,

$$\mathcal{L}_{\rm int} = -gm(t)\phi(x), \tag{3.10}$$

where $m(t)$ is the monopole moment of the detector and g a coupling constant. At the first order of perturbation theory, the transition amplitude from the ground state, $|E_0\rangle\otimes|\Omega\rangle$ (where $|E_0\rangle$ denotes the ground state of the detector with energy E_0 and $|\Omega\rangle$ denotes the ground state of the scalar field) to a state $|E\rangle\otimes|\Psi\rangle$ (where $|E\rangle$ is an excited state of the detector with energy $E>E_0$), is given by,

$$\mathcal{A}(E_0\to E) = ig\int_{-\infty}^{\infty}\langle E|\hat{m}(\tau)|E_0\rangle\langle\Psi|\hat{\phi}(x(\tau))\mathrm{d}\tau|\Omega\rangle, \tag{3.11}$$

where τ is the geodesic time and $x^\mu(\tau)$ parametrizes a geodesic. The probability P that the detector transits from E_0 to E is obtained by squaring the transition amplitude, and summing over all intermediate (excited) states of the field $|\Psi\rangle$, resulting in,

$$P = g^2\sum_E|\langle E|\hat{m}(0)|E_0\rangle|^2\mathcal{F}(\Delta E), \tag{3.12}$$

where we made use of, $\hat{m}(0)=\mathrm{e}^{-i\hat{H}_0\tau}\hat{m}(\tau)\mathrm{e}^{i\hat{H}_0\tau}$, denoting the monopole moment evolved back to the initial time $\tau=0$, and $\mathcal{F}(\Delta E)$ denotes the response function of the detector given by,

$$\mathcal{F}(\Delta E) = \int_{-\infty}^{\infty}\mathrm{d}\tau\int_{-\infty}^{\infty}\mathrm{d}\tau'\mathrm{e}^{-i\Delta E(\tau-\tau')}i\Delta^{(+)}\left(x^\mu(\tau);x^\nu(\tau')\right), \qquad \Delta E = E-E_0. \tag{3.13}$$

Here $i\Delta^{(+)}\left(x^\mu(\tau);x^\nu(\tau')\right)$ is the positive frequency Wightman function (2.4) evaluated along the geodesics of the detector,

$$x^\mu = x^\mu(\tau), \qquad x'^\nu = x^\nu(\tau'). \tag{3.14}$$

It is useful to transform the integrals in equation (3.13) to the relative and average proper times, $\Delta\tau=\tau-\tau'$ and $T=(\tau+\tau')/2$,

$$\mathcal{F}(\Delta E) = \int_{-\infty}^{\infty}\mathrm{d}T\int_{-\infty}^{\infty}\mathrm{d}\Delta\tau\mathrm{e}^{-i\Delta E\Delta\tau}i\Delta^{(+)}\left(x^\mu(T+\Delta\tau/2);x^\nu(T-\Delta\tau/2)\right), \tag{3.15}$$

such that one can define the *transition rate* $\mathcal{R}$ as the rate of detector's transitions, $E_0\to E$, per unit time,

$$\begin{aligned}\mathcal{R}(T,\Delta E) &= \lim_{\Delta T\to 0}\left[\frac{\Delta\mathcal{F}(\Delta E)}{\Delta T}\right]\\ &= \int_{-\infty}^{\infty}\mathrm{d}\Delta\tau\mathrm{e}^{-i\Delta E\Delta\tau}i\Delta^{(+)}\left(x^\mu(T+\Delta\tau/2);x^\nu(T-\Delta\tau/2)\right).\end{aligned} \tag{3.16}$$

Strictly speaking this transition rate is valid only for eternal gravitational waves. Realistic gravitational waves are transients with a finite duration ΔT, suggesting that the integration limits for $\Delta\tau$ should be placed roughly at $\pm\Delta T/2$. However, due to the oscillatory character of the integrand (generated by the factor $\mathrm{e}^{-i\Delta E\Delta\tau}$), which is responsible for a destructive

interference at large $\Delta\tau$'s, as long as $\Delta E\Delta T \gg 1$, the finite limits of integration will not significantly affect the integral in (3.16), and thus we shall neglect it in what follows; for a more comprehensive discussion of this point see [16].

Now, from equations (3.6)–(3.8) one easily obtains,

$$\Delta u(\tau) = 2P_v\Delta\tau, \qquad (\Delta u_0 = 0), \tag{3.17}$$

$$\Delta x^i(\tau) = \frac{\Delta u}{2P_v}\mathcal{G}^{ij}(u;u')P_j, \qquad (i,j=1,2,\cdots,D-2,\ \Delta x^i_0 = 0), \tag{3.18}$$

$$\Delta v = \frac{\Delta u}{4P_v^2}\Big[1 + P_i\mathcal{G}^{ij}(u;u')P_j\Big], \qquad (\Delta v_0 = 0), \tag{3.19}$$

where $\Delta x^\mu_0 = 0$ follows from the fact that we are considering worldlines of a single particle. From equation (3.17) we see that the conserved momentum $2P_v$ converts a proper time interval $\Delta\tau$ into the coordinate time interval Δu. When these are inserted into equation (2.5) one obtains,

$$\begin{aligned}\Delta\bar{x}^2_{(\pm)}(x;x') &= -(\Delta u\mp i\epsilon)\left[\frac{\Delta u}{4P_v^2}\left(1 + P_i\mathcal{G}^{ij}(u;u')P_j\right)\mp i\epsilon\right]\\ &\quad + \left(\frac{\Delta u}{2P_v}\mathcal{G}^{ik}(u;u')P_k\right)\mathcal{G}_{ij}(u;u')\left(\frac{\Delta u}{2P_v}\mathcal{G}^{jl}(u;u')P_l\right)\\ &= -\frac{(\Delta u\mp i\epsilon)^2}{4P_v^2} = -(\Delta\tau\mp i\epsilon)^2 = -\frac{(\Delta t\mp i\epsilon)^2}{E^2},\end{aligned} \tag{3.20}$$

where, for gravitational waves oscillating in the $(i,j=x,y)$-plane, we have,

$$\mathcal{G}_{ij}(u;u') \equiv \begin{cases}\mathcal{G}^{\perp}_{ij}(u;u'), & \text{when} \quad i,j=1,2\\ \delta_{ij}, & \text{when} \quad i,j=3,\cdots,D-2\,.\end{cases} \tag{3.21}$$

Equation (3.20) implies that, transforming from lightcone coordinates to Cartesian coordinates is simple, and it amounts to, $(\Delta u\mp i\epsilon)/(2P_v)\to(\Delta t\mp i\epsilon)/E$, where E is the energy per unit mass. Equation (3.20) is a remarkable result, and it states that the only effect planar gravitational waves induce on inertial particles (moving along free geodesics) as seen by an Unruh–DeWitt detector is through the prefactor in the Wightman function (3.24). Now upon inserting equation (2.4) into (3.15) one obtains,

$$\mathcal{R}(U,\Delta E) = \frac{\hbar m^{D-2}}{(2\pi)^{\frac{D}{2}}}\int_{-\infty}^{\infty}\frac{\mathrm{d}\Delta\tau}{[\gamma(u)\gamma(u')]^{\frac{1}{4}}\sqrt{\det[\mathcal{G}^{ij}(U;\Delta u)]}}\mathrm{e}^{-i\Delta E\Delta\tau}\frac{K_{\frac{D-2}{2}}\left(im(\Delta\tau-i\epsilon)\right)}{\left(im(\Delta\tau-i\epsilon)\right)^{\frac{D-2}{2}}}, \tag{3.22}$$

where $u = U+\Delta u/2$, $u' = U-\Delta u/2$, and we made use of equation (3.20), and we made use of, $m\sqrt{-(\Delta\tau-i\epsilon)^2} = im(\Delta\tau-i\epsilon)$. Note that in equation (3.22) we use the standard $i\epsilon$ prescription on the Wightman function to describe detector's response rate, which is suitable for problems in which the coupling between the detector and the system is time independent, or when it is turned on adiabatically in time. In more complicated situations, for example, when the gravitational wave amplitude varies in time, a more careful analysis is needed, see e.g. [17].

The principal objective of this section is to compute the transition rate in equation (3.22). Except for the factor $\left[\sqrt{\gamma(u)\gamma(u')}\det[\mathcal{G}^{ij}(U;\Delta u)]\right]^{-\frac{1}{2}}$, the integrand in equation (3.22) is identical to that for the massive scalar field in Minkowski vacuum. Since in the on-shell limit (when $u'=u$) this factor equals unity, the effect is purely off-shell, i.e. it occurs due to the

off-shell modification of the surface area in which the gravitational waves propagate[2]. The effect is purely off-shell, as it arises as the result of quantum superposition of a single massive scalar particle (the detector) moving on two distinct trajectories, which propagate in a space in which the distances in the plane of propagation are contracted (or expanded) by the gravitational backreaction induced by gravitational waves. Since the transitions arise as a result of quantum superposition of different trajectories, the effect is purely quantum mechanical, and therefore it can be considered as a dynamical analogue of the quantum gravitational effect discussed e.g. in references [18, 19].

Before we embark on the full calculation, let us firstly consider the simpler, massless scalar, case, whose Wightman function is obtained by taking the limit $m \to 0$ in equation (2.4). The following series representation of the Bessel function is handy,

$$\frac{K_\nu(z)}{z^\nu} = \frac{\Gamma(\nu)\Gamma(1-\nu)}{2^{1+\nu}}\left[\sum_{n=0}^{\infty}\frac{(z/2)^{2n-2\nu}}{n!\Gamma(n+1-\nu)} - \sum_{n=0}^{\infty}\frac{(z/2)^{2n}}{n!\Gamma(n+1+\nu)}\right], \quad (3.23)$$

where $z = m\sqrt{\Delta\bar{x}^2_{(\pm)}}$ and $\nu = (D-2)/2$. In the massless limit only the first term of the first series in equation (3.23) contributes, resulting in,

$$i\Delta_0^{(+)}(x;x') = \frac{\hbar\Gamma(\frac{D-2}{2})}{4\pi^{D/2}[\gamma(u)\gamma(u')]^{1/4}\sqrt{\det[\mathcal{G}^{ij}(u;u)]}}\left(\frac{1}{\Delta\bar{x}^2_{(+)}(x;x')}\right)^{\frac{D-2}{2}}, \quad (3.24)$$

where $\Delta\bar{x}^2_{(+)}(x;x') = -(\Delta\tau - i\epsilon)^2$ is given in equation (3.20), and whose four dimensional limit is obtained by setting $D=4$.

In what follows we evaluate the integral in equation (3.22) for two simple cases of monochromatic gravitational waves. We shall firstly consider the detector transition rate for monochromatic, circularly polarized gravitational waves, and then for maximally polarized gravitational waves. In this paper we calculate detector's excitation rate, for which $\Delta E = E - E_0 > 0$. Namely, in realistic situations one expects miniscule detector rates, and since the excitation rate of the detector in Minkowski vacuum is exactly zero, observing any *non-vanishing detector's excitation rate* could be interpreted as a signal for passing gravitational waves.

3.3. Monochromatic circularly polarized gravitational waves

The deformation matrix (3.21) for gravitational waves in linear representation (1.2) in the $(xy)-$plane in the $\{U,\Delta u\}-$coordinates, $\mathcal{G}^\perp_{ij}(U;\Delta u)$, can be inferred from equations (2.10) and (2.11),

$$\mathcal{G}^\perp_{ij}(U;\Delta u) = \frac{\det[\mathcal{G}^\perp_{ij}(\Delta u)]}{\gamma}\begin{pmatrix} 1+h\cos(\omega_g U)j_0\left(\frac{\omega_g\Delta u}{2}\right) & h\sin(\omega_g U)j_0\left(\frac{\omega_g\Delta u}{2}\right) \\ h\sin(\omega_g U)j_0\left(\frac{\omega_g\Delta u}{2}\right) & 1-h\cos(\omega_g U)j_0\left(\frac{\omega_g\Delta u}{2}\right)\end{pmatrix}$$
$$= \frac{\mathcal{G}_\perp(\Delta u)}{\gamma}\left[\delta^\perp_{ij} + h^\perp_{ij}(U)j_0\left(\frac{\omega_g\Delta u}{2}\right)\right], \qquad (i,j=1,2), \quad (3.25)$$

[2] By the surface in which the gravitational waves propagate we mean the surface orthogonal to the direction of propagation, i.e. it is the xy-plane for the waves propagating in the z-direction. The off-shell modification of the surface area for circularly polarized gravitational waves is illustrated in figure 3 of [1].

$$\gamma\mathcal{G}_{\perp}^{-1}(\Delta u)\equiv\gamma\det\left[\mathcal{G}^{ij}(U;\Delta u)\right]=\frac{1}{\gamma}\left[1-h^2j_0^2\Big(\frac{\omega_g\Delta u}{2}\Big)\right],\qquad(\gamma=1-h^2),\tag{3.26}$$

where $U=(u+u')/2$, $\Delta u=u-u'$, and $j_0(z)=\sin(z)/z$[3]. For circularly polarized gravitational waves the transition rate in equation (3.22) simplifies to,

$$\mathcal{R}(\Delta E)=\frac{\hbar m^{D-2}\sqrt{\gamma}}{(2\pi)^{\frac{D}{2}}}\int_{-\infty}^{\infty}\frac{\mathrm{d}\Delta\tau}{\left[1-h^2j_0^2\left(P_v\omega_g\Delta\tau\right)\right]^{1/2}}\mathrm{e}^{-i\Delta E\Delta\tau}\frac{K_{\frac{D-2}{2}}\left(im(\Delta\tau-i\epsilon)\right)}{\left(im(\Delta\tau-i\epsilon)\right)^{\frac{D-2}{2}}},\tag{3.27}$$

where we made use of, $\Delta u=2P_v\Delta\tau$. Notice that, for circularly polarized gravitational waves, $\mathcal{R}(\Delta E)$ does not depend on the average time U. When understood as a function of complex Δu, the integrand in equation (3.27) has two square-root cuts along the imaginary axis of complex $\Delta\tau$, starting at the roots of the equation,

$$j_0\left(P_v\omega_g\Delta\tau\right)=\frac{\sinh(\theta)}{\theta}=\frac{1}{h}\gg1,\tag{3.28}$$

where $\theta=-iP_v\omega_g\Delta\tau$. For $h\ll1$ the root $\theta_0(h)$ can be approximated by the solution of $\theta_0/(\mathrm{e}^{\theta_0}-\mathrm{e}^{-\theta_0})=h/2\ll1\Rightarrow(-|\theta_0|)\mathrm{e}^{-|\theta_0|}\approx-h/2$, which can be expressed in terms of the Lambert W function (defined by the solution of, $w\mathrm{e}^w=z$)[4],

$$|\theta_0(h)|\approx-\Re\left[W\left(-\frac{h}{2}\right)\right],\tag{3.29}$$

such that there are two symmetric solutions[5]. These two roots define the beginning of the square-root cuts, the lower one is shown in figure 1. The lower cut is responsible for the detector's excitation rate, for which $\Delta E=E-E_0>0$, which is the rate which will be calculated in this paper[6]. The cuts are located at the imaginary $\Delta\tau$-axis, which correspond to spacelike separations, and they are generated by the coupling between the massive scalar and the gravitational waves; the cuts (rather than poles) arise as a result of the resummed graviton insertions.

One can make use of the Cauchy integral formula to replace the integral in equation (3.27) by an equivalent integral,

[3] In exponential representation used in [1], in which the spatial part of the metric tensor is, $g_{ij}(u)=[\exp(\mathbf{\hbar}(u))]_{ij}$, we have, $\gamma\equiv\det[g_{ij}(u)]=1$ and $\gamma\Upsilon(u;u')=\cosh^2(\tilde{h})-\sinh^2(\tilde{h})j_0^2(\omega_g\Delta u/2)$, such that $\gamma\Upsilon(u;u)=1$.

[4] The solutions for the poles, $|\theta_0|\approx-\Re[W(-h/2)]$ can be approximated by iterating, $|\theta_0|=\ln\left(\frac{2}{h}\right)+\ln(|\theta_0|)$, giving $|\theta_0|=\ln\left(\frac{2}{h}\right)+\ln\left[\ln(\frac{2}{h})+\ln\left(\ln(\frac{2}{h})\cdots\right)\right]$. The exact solution can be obtained by iterating, $|\theta_0|=\ln\left(\frac{2}{h}\right)+\ln\left(\frac{|\theta|}{2}+\sqrt{h^2+\theta_0^2}\right)$. When $h\ll1$, the error in the approximation by the Lambert function decreases as, $\mathcal{O}(h^2/\ln^2(h))$, such that, in the limit when $h\to0$, the approximation by the (real part of the) Lambert function becomes exact.

[5] In exponential representation the approximate roots are given by changing equation (3.29) to $|\theta_0(h)|\approx-\Re[W(-\tanh(\tilde{h})/2)]$. This means that the results in exponential representation are obtained from those in linear representation by the replacement, $h\to\tanh(\tilde{h})$.

[6] If one were interested in detector's de-excitation rate stimulated by passing gravitational waves, for which $\Delta E<0$, the complex contour would have to be closed in the upper-half complex Δu plane. The relevant contributions to the rate would then come not only from the cut above the real axis, but also from the pole at $\Delta\tau=i\epsilon$. Since this pole contributes also in Minkowski space, it would be hard to disentangle the pole contributions from those generated by the cut, and for that reason we do not study these transitions here. Note that the *cut* contribution to the *de-excitation rate* can be obtained from the cut contribution to the excitation rate simply by exacting the replacement, $\Delta E\to|\Delta E|$, in the rates.

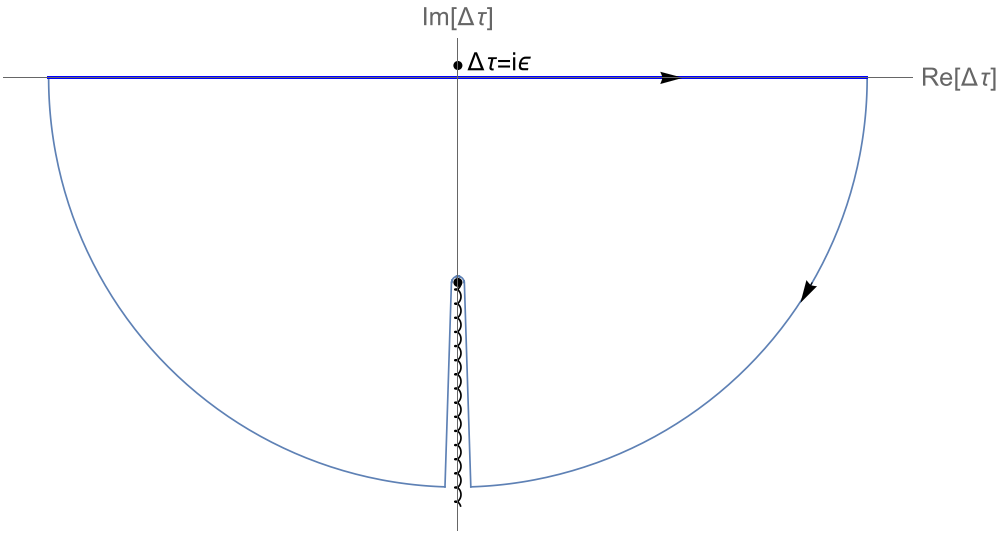

Figure 1. The complex contour used to obtain the detector excitation rate in equation (3.16), which shows that the integral over the real axis can be replaced by the two sections along the cut in the lower complex Δu-plane.

$$\mathcal{R}(\Delta E)=\frac{\hbar m\sqrt{\gamma}}{2\pi^2}\int_{\theta_0}^{\infty}\frac{\mathrm{d}\theta}{\left[h^2\sinh^2(\theta)-\theta^2\right]^{1/2}}\mathrm{e}^{-\frac{\Delta E}{P_v\omega_g}\theta}K_1\left(\frac{m}{P_v\omega_g}\theta\right), \tag{3.30}$$

where we set $D=4$, which is allowed as the integral in equation (3.30) is finite in $D=4$, and therefore it does not need to be regularized. The parameter $\theta_0>0$ in equation (3.30) is the positive root of equation (3.29), we made use of the fact that the integral over the entire contour in figure 1 vanishes and, in the last step, made the replacement, $\theta\to-\theta$. In the massless limit equation (3.30) reduces to,

$$\mathcal{R}(\Delta E)=\frac{\hbar\sqrt{\gamma}P_v\omega_g}{2\pi^2}\int_{\theta_0}^{\infty}\frac{\mathrm{d}\theta}{\theta\left[h^2\sinh^2(\theta)-\theta^2\right]^{1/2}}\mathrm{e}^{-\frac{\Delta E}{P_v\omega_g}\theta}. \tag{3.31}$$

The integrals in equations (3.30) and (3.31) are hard, and cannot be evaluated analytically. Let us firstly consider the easier, massless case.

Two analytic approximations can be used for the transition rate in equation (3.27), an expansion in powers of h^2 and an expansion around the beginning of the cut, the latter increasing in accuracy in the large energy limit, when $\Delta E\gg P_v\omega_g$. The first approximation amounts to setting $D=4$ and expanding (3.27) in powers of h^2. This replaces the cut contribution by a sum over the poles at $\Delta u=i\epsilon$ of the order $2n+2$,

$$\mathcal{R}(\Delta E)=\frac{\hbar m^2\sqrt{\gamma}}{4\pi^2}\frac{1}{\sqrt{\pi}}\sum_{n=1}^{\infty}\Gamma\left(n+\frac{1}{2}\right)\frac{h^{2n}}{n!}\int_{-\infty}^{\infty}\frac{\mathrm{d}\Delta\tau}{(P_v\omega_g\Delta\tau)^{2n}}\sin^{2n}(P_v\omega_g\Delta\tau)\mathrm{e}^{-i\Delta E\Delta\tau}$$
$$\times\frac{K_1\left(im(\Delta\tau-i\epsilon)\right)}{im(\Delta\tau-i\epsilon)}, \tag{3.32}$$

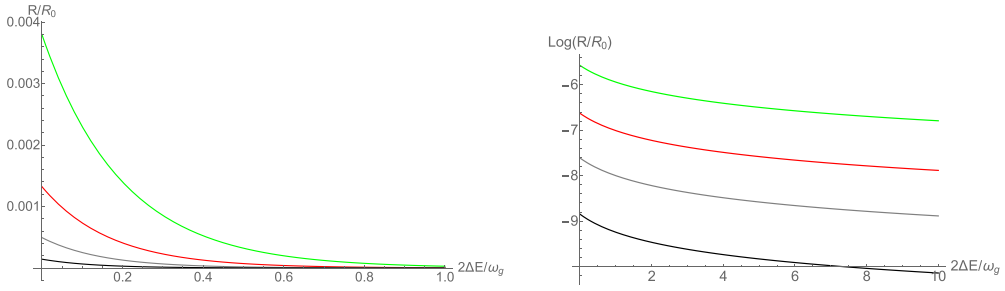

Figure 2. *Left panel:* The transition rate $\mathcal{R}$ in equation (3.31) for a massless scalar as a function of $\Delta E/(P_v\omega_g)$ in units of $\mathcal{R}_0=\hbar\sqrt{1-h^2}P_v\omega_g/(2\pi^2)$ as measured by the Unruh–DeWitt detector. Different curves are for different values of the gravitational strain (from top down): $h=0.1$ (green), $h=0.05$ (red), $h=0.025$ (gray), and $h=0.01$ (black). *Right panel:* The same diagram for $\ln(\mathcal{R}/\mathcal{R}_0)+\Delta E\theta_0/(P_v\omega_g)$, where $\theta_0>0$ is the imaginary pole at the beginning of the square root cut in equation (3.28).

which can be evaluated by making use of the Cauchy integral formula. The integration of the nth term in the sum does not vanish provided $\Delta E-2nP_v\omega_g<0$. In the massless limit the last term in equation (3.27) simplifies to, $-1/[m(\Delta\tau-i\epsilon)]^2$, such that the integral evaluates to,

$$\mathcal{R}(\Delta E)=\frac{\hbar\sqrt{\gamma}P_v\omega_g}{2\pi^2}\left\{\frac{\pi}{6}h^2\left(1-\frac{\Delta E}{2P_v\omega_g}\right)^3\Theta(2P_v\omega_g-\Delta E)+\frac{\pi}{5}h^4\left[-\frac{1}{8}\left(1-\frac{\Delta E}{2P_v\omega_g}\right)^3\right.\right.$$
$$\left.\left.\times\,\Theta(2P_v\omega_g-\Delta E)+\left(1-\frac{\Delta E}{4P_v\omega_g}\right)^3\Theta(4P_v\omega_g-\Delta E)\right]+\mathcal{O}(h^6)\right\}, \tag{3.33}$$

where we made use of, $\sin^2(z)=\frac{1}{2}-\frac{1}{4}\left(\mathrm{e}^{2iz}+\mathrm{e}^{-2iz}\right)$, and we have assumed that, $\Delta E>0$ and $P_v>0$.

The second analytic approximation can be obtained by expanding the integrand in equation (3.31) around the beginning of the cut. The result is,

$$\mathcal{R}(\Delta E)\approx\frac{\hbar\sqrt{\gamma}P_v\omega_g}{2\pi^2}\sqrt{\frac{P_v\omega_g}{\Delta E}}\left(\frac{h}{2}\right)^{\frac{\Delta E}{P_v\omega_g}}\frac{1}{\left[\ln\left(\frac{2}{h}\right)+\ln\left(\ln\left(\frac{2}{h}\right)\right)\right]^{2+\frac{\Delta E}{P_v\omega_g}}}\left[1+\mathcal{O}\left(\frac{P_v\omega_g}{\Delta E}\right)\right]. \tag{3.34}$$

One can evaluate equation (3.31) numerically, and the results are shown in figure 2. In figure 3 we compare the numerical results for the transition rate with two analytical approximations. The first approximation is obtained by expanding in powers of h^2 (dashed lines in figure 3) and the second by expanding around the beginning of the cut (dotted lines in figure 3). Both approximations are reasonable, but neither is accurate. The second approximation captures correctly the large ΔE behavior, $\mathcal{R}(\Delta E)\propto\exp\left[-\frac{\Delta E}{P_v\omega_g}\theta_0\right]$, meaning that the transition rate is exponentially suppressed with growing $\left[\frac{\Delta E}{P_v\omega_g}\theta_0\right]$, but the analytical estimate poorly approximates the constant in front of the exponential. Due to the complicated dependence of $\theta_0(h)$ on h in equation (3.29), the dependence of the transition rate on h is nonanalytic, which explains why expanding in powers of h^2 performs relatively poorly. This kind of nonanalytic behavior is hard to guess, and impossible to obtain without knowing the scalar Wightman function from [1], which resums the gravitational wave insertions.

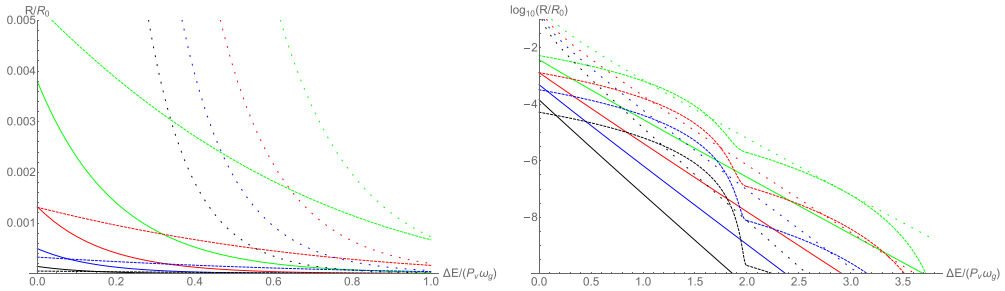

Figure 3. *Left panel:* The detector transition rate $\mathcal{R}$ for a massless scalar as a function of $\Delta E/(P_v\omega_g)$ in units of $\mathcal{R}_0=\hbar\sqrt{1-h^2}P_v\omega_g/(2\pi^2)$ as measured by the Unruh–DeWitt detector. Different curves are for different values of the gravitational strain: $h=0.1$ (green), $h=0.05$ (red), $h=0.025$ (blue), and $h=0.01$ (black). Solid lines show numerical results, dashed lines are approximate curves in equation (3.33), obtained by expanding the integrand in powers of h^2, and dotted lines represent the function in equation (3.34), obtained by expanding the integrand around the beginning of the cut. *Right panel:* The same diagram for $\log_{10}(\mathcal{R}/\mathcal{R}_0)$.

Switching on the scalar mass suppresses the transition rate further, and the results obtained by numerically integrating (3.30) for $m=P_v\omega_g$ shown in figure 4 are significantly suppressed when compared with those for the massless scalar in figures 2 and 3. Just as in the massless case, at large ΔE, the results decay exponentially as, $\mathcal{R}\propto\exp\left[-\frac{\Delta E}{P_v\omega_g}\theta_0\right]$, and in the limit of a large mass, $m\theta_0\gg P_v\omega_g$, there is an additional exponential suppression, $\mathcal{R}\propto\exp\left[-\frac{(\Delta E+m)}{P_v\omega_g}\theta_0\right]$. To see that, let us approximately evaluate the integral in equation (3.30) by expanding around the beginning of the cut at $\theta=\theta_0(h)$,

$$\mathcal{R}(\Delta E)=\frac{\hbar\sqrt{\gamma}m}{2\pi^2}\sqrt{\frac{\pi P_v\omega_g}{2\Delta E\theta_0(\theta_0-1)}}K_1\left(\frac{m\theta_0}{P_v\omega_g}\right)\mathrm{e}^{-\frac{\Delta E\theta_0}{P_v\omega_g}}$$
$$\times\left\{1-\frac{P_v\omega_g}{2\Delta E}\left[\frac{2\theta_0^2-1}{4\theta_0(\theta_0-1)}+\frac{m}{P_v\omega_g}\frac{K_2\left(\frac{m\theta_0}{P_v\omega_g}\right)}{K_1\left(\frac{m\theta_0}{P_v\omega_g}\right)}-\frac{1}{\theta_0}\right]+\mathcal{O}(\Delta E^{-2})\right\},\qquad(3.35)$$

which applies when $\Delta E\theta_0/(P_v\omega_g)\gg1$, and where we dropped the term $h^2/(2\theta_0)$ in the expansion, $\sqrt{\theta_0^2+h^2}\simeq\theta_0+\mathcal{O}(h^2/\theta_0)$. This amounts to approximating the position of the cut, $\theta=\theta_0(h)$, by the Lambert function in equation (3.29). We shall not attempt to evaluate the integrals in equation (3.32) for the massive case, as that would require not only to account for the contributions of the poles at $\Delta u=i\epsilon$, but also for the contribution of the logarithmic cut of the modified Bessel function, $im(\Delta u-i\epsilon)K_1\left(im(\Delta u-i\epsilon)\right)$, which extends from $\Delta u=0$ to $0+i\infty$. Finally, in figure 5 we show the same transition rate as in figure 4, but now as a function of the mass for a fixed $\Delta E=2P_v\omega_g$ (left panel) and $\Delta E=10P_v\omega_g$ (right panel). The figure shows that the transition rate is exponentially suppressed by the mass as, $\mathcal{R}\sim\mathrm{e}^{-m\theta_0(h)/(P_v\omega_g)}$, which can be also inferred from the asymptotic expansion of the Bessel function in equation (3.35), $K_1\left(\frac{m\theta_0}{P_v\omega_g}\right)\sim\sqrt{\frac{\pi P_v\omega_g}{2m\theta_0}}\exp\left(-\frac{m\theta_0}{P_v\omega_g}\right)$.

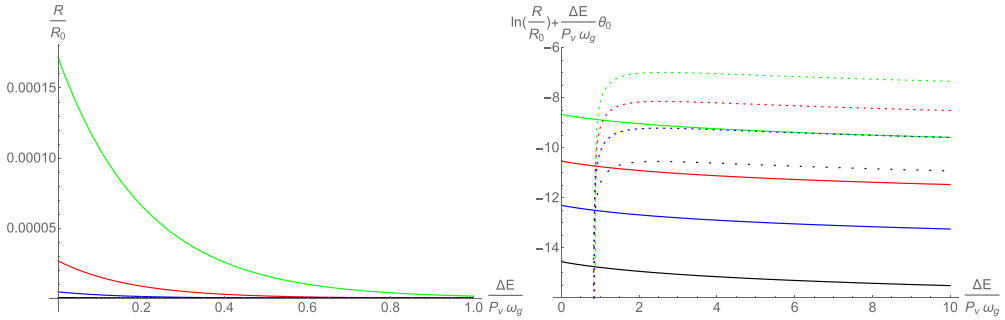

Figure 4. *Left panel:* The detector transition rate $\mathcal{R}(\Delta E)$ for a massive scalar with $m=P_v\omega_g$ as a function of $\Delta E/(P_v\omega_g)$ in units of $\mathcal{R}_0=\hbar\sqrt{1-h^2}P_v\omega_g/(2\pi^2)$ as measured by the Unruh–DeWitt detector. Different curves are for different values of the gravitational strain: $h=0.1$ (green), $h=0.05$ (red), $h=0.025$ (blue), and $h=0.01$ (black). *Right panel:* The same diagram for $\ln(\mathcal{R}/\mathcal{R}_0)+(\Delta E\theta_0)/(P_v\omega_g)$.

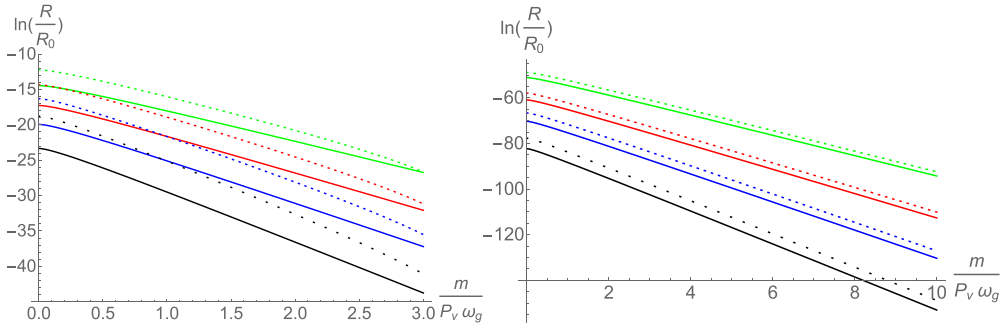

Figure 5. *Left panel:* The detector transition rate $\mathcal{R}$ for a massive scalar with $\Delta E/(P_v\omega_g)=2$ as a function of $m/(P_v\omega_g)$ in units of $\mathcal{R}_0=\hbar\sqrt{1-h^2}P_v\omega_g/(2\pi^2)$ as measured by the Unruh–DeWitt detector. Different curves are for different values of the gravitational strain: $h=0.1$ (green), $h=0.05$ (red), $h=0.025$ (blue), and $h=0.01$ (black). *Right panel:* The same but with with $\Delta E/(P_v\omega_g)=10$. The solid curves are numerical results, and the short dashed curves are the approximation in equation (3.35).

3.4. Monochromatic elliptically polarized gravitational waves

Here we shall consider general elliptically polarized gravitational waves, whose analysis is much trickier, as the interaction with the detector depends on the average time variable, $U=(u+u')/2$. Let us begin our analysis by noting that equation (2.8) can be recast as,

$$\mathcal{G}^{ij}(U,\Delta u)=\sum_{n=0}^{\infty}\left[\frac{\partial^{2n}}{\partial U^{2n}}g^{ij}(U)\right]\frac{(\Delta u/2)^{2n}}{(2n+1)!}, \tag{3.36}$$

where $\Delta u=u-u'$, and $g^{ij}(U)$ denotes the inverse of $g_{ij}(U)$, which for generally polarized waves (fluctuating in a two-dimensional plane) takes the form (cf equation (2.9)),

$$g^{ij}(U)=\frac{1}{1-h_+^2c_+^2-h_\times^2c_\times^2}\begin{pmatrix}1-h_+c_+ & -h_\times c_\times\\ -h_\times c_\times & 1+h_+c_+\end{pmatrix}, \tag{3.37}$$

where $c_+(U)=\cos(\omega_g U+\psi/2)$, $c_\times(U)=\cos(\omega_g U-\psi/2)$, where ψ is an arbitrary phase (in the case of nonpolarized gravitational waves, $\psi=\pi/2$). Evaluating (3.36) for g^{ij} in equation (3.37) is a formidable task, and we shall content ourselves by evaluating $\mathcal{G}^{ij}(u;u')$ to the quadratic order in h_+ and $h_\times$,

$$\mathcal{G}^{ij}(U,\Delta u)=\begin{pmatrix}1&0\\0&1\end{pmatrix}\biggl[1+\frac{h_+^2}{2}\Bigl(1+(2c_+^2-1)j_0(\omega_g\Delta u)\Bigr)+\frac{h_\times^2}{2}\Bigl(1+(2c_\times^2-1)j_0(\omega_g\Delta u)\Bigr)\biggr]$$
$$+\begin{pmatrix}-h_+c_+&-h_\times c_\times\\-h_\times c_\times&h_+c_+\end{pmatrix}j_0\biggl(\frac{\omega_g\Delta u}{2}\biggr)+\mathcal{O}(h_+^2h_\times,h_+h_\times^2),\qquad(3.38)$$

whose determinant equals,

$$\mathcal{G}^{-1}(U;\Delta u)=1-h_+^2\biggl[c_+^2j_0^2\biggl(\frac{\omega_g\Delta u}{2}\biggr)-1-(2c_+^2-1)j_0(\omega_g\Delta u)\biggr]$$
$$-h_\times^2\biggl[c_\times^2j_0^2\biggl(\frac{\omega_g\Delta u}{2}\biggr)-1-(2c_\times^2-1)j_0(\omega_g\Delta u)\biggr]+\mathcal{O}(h_+^2h_\times,h_+h_\times^2).\qquad(3.39)$$

In the circularly polarized case, in which $\psi=\pi/2$ and $h_+=h_\times=h$, this reduces to, $\mathcal{G}^{-1}(U;\Delta u)\to 1-h^2\Bigl[j_0^2\Bigl(\frac{\omega_g\Delta u}{2}\Bigr)+2\Bigr]$, which agrees with equation (3.26) when one recalls that, $1/\gamma^2=1+2h^2+\mathcal{O}(h^4)$. Upon introducing $\tilde\gamma(h_+,h_\times)=1-\frac{h_+^2+h_\times^2}{2}$, equation (3.39) can be recast as,

$$\mathcal{G}^{-1}(U;\Delta u)=\frac{1}{\tilde\gamma^2}\biggl\{1-\biggl[\bigl(h_+^2c_+^2+h_\times^2c_\times^2\bigr)j_0^2\biggl(\frac{\omega_g\Delta u}{2}\biggr)-\bigl(h_+^2(2c_+^2-1)$$
$$+h_\times^2(2c_\times^2-1)\bigr)j_0(\omega_g\Delta u)\biggr]\biggr\}+\mathcal{O}(h_+^2h_\times,h_+h_\times^2).\qquad(3.40)$$

To complete the analysis, we also need,

$$\sqrt{\gamma(u)\gamma(u')}=\tilde\gamma-\frac{1}{2}\bigl(h_+^2(2c_+^2-1)+h_\times^2(2c_\times^2-1)\bigr)\cos(\omega_g\Delta u)+\mathcal{O}(h_+^2h_\times,h_+h_\times^2),\qquad(3.41)$$

which, when multiplied with (3.40), gives,

$$\sqrt{\gamma(u)\gamma(u')}\mathcal{G}^{-1}(U;\Delta u)=\frac{1}{\tilde\gamma}\biggl\{1-\biggl[\bigl(h_+^2c_+^2+h_\times^2c_\times^2\bigr)j_0^2\biggl(\frac{\omega_g\Delta u}{2}\biggr)-\bigl(h_+^2(2c_+^2-1)$$
$$+h_\times^2(2c_\times^2-1)\bigr)\Bigl(j_0(\omega_g\Delta u)-\frac{1}{2}\cos(\omega_g\Delta u)\Bigr)\biggr]\biggr\}$$
$$+\mathcal{O}(h_+^2h_\times,h_+h_\times^2).\qquad(3.42)$$

This product appears in the propagator in equation (3.22), and generates square-root cuts[7], just as in the circularly polarized waves in equation (3.27). The integral can be evaluated by contour integration, with the contour showed in figure 1, resulting in the cut contribution (cf equation (3.30)),

$$\mathcal{R}(U,\Delta E)=\frac{\hbar m\sqrt{\tilde\gamma}}{2\pi^2}\int_{\theta_0}^\infty\frac{\mathrm{d}\theta}{\bigl[H^2(U,\theta)-\theta^2\bigr]^{1/2}}\mathrm{e}^{-\frac{\Delta E}{P_v\omega_g}\theta}K_1\biggl(\frac{m}{P_v\omega_g}\theta\biggr),\qquad(3.43)$$

[7] Our analysis is accurate at the order h^2, and thus not exact. Therefore, one should be aware of the possibility that polarized gravitational wave may generate more baroque cuts in the complex Δu plane, for an illustration see appendix B.

where $h^2(U) = h_+^2 c_+^2(U) + h_\times^2 c_\times^2(U)$,

$$H^2(U,\theta) = h^2(U)\sinh^2(\theta) + \left[h^2(U) - \frac{h_+^2+h_\times^2}{2}\right]\left[\theta^2\cosh(2\theta) - \theta\sinh(2\theta)\right], \tag{3.44}$$

and $\theta_0 > 0$ denotes the beginning of the cut defined by, $H^2(U,\theta_0) = \theta_0^2$. Next we insert,

$$h^2(U) = \frac{h_+^2+h_\times^2}{2} + \frac{h_+^2+h_\times^2}{2}\cos(2\omega_g U)c_\psi - \frac{h_+^2-h_\times^2}{2}\sin(2\omega_g U)s_\psi,$$
$$(c_\psi = \cos(\psi),\ s_\psi = \sin(\psi)), \tag{3.45}$$

into equation (3.44) to obtain,

$$\left[\frac{h_+^2+h_\times^2}{2}c_\psi\cos(2\omega_g U) - \frac{h_+^2-h_\times^2}{2}s_\psi\sin(2\omega_g U)\right]$$
$$\times\left[\sinh^2(\theta_0) + \theta_0^2\cosh(2\theta_0) - \theta_0\sinh(2\theta_0)\right] + \frac{h_+^2+h_\times^2}{2}\sinh^2(\theta_0) - \theta_0^2 = 0. \tag{3.46}$$

Because of the U dependence, equation (3.46) may or may not have a solution, meaning that the cuts exist only when (3.46) can be solved for some real U. To simplify our analysis, recall that we are interested in the limit when, $h_+, h_\times \ll 1$, in which case in most of the parameter space $\theta_0 \gg 1$, and one can approximate equation (3.46) by keeping the leading order terms $\propto \mathrm{e}^{2\theta_0}$ only[8]. Multiplying equation (3.46) by $2\mathrm{e}^{-2\theta_0}/\cos^2(\omega_g U) = 2\mathrm{e}^{-2\theta_0}(1+t^2)$ and neglecting the terms suppressed as $\sim \mathrm{e}^{-2n\theta_0}$ $(n = 1,2)$ yields a quadratic equation for $t = \tan(\omega_g U)$,

$$at^2 - 2bt + c > 0 \implies a(t-t_+)(t-t_-) > 0, \quad t_\pm = \frac{1}{a}\left[b \pm \sqrt{\Delta}\right], \qquad \Delta = b^2 - ac, \tag{3.47}$$

where

$$a = \frac{h_+^2+h_\times^2}{2}\left[-\left(\theta_0^2-\theta_0+\frac{1}{2}\right)c_\psi + \frac{1}{2}\right], \quad b = \frac{h_+^2-h_\times^2}{2}\left(\theta_0^2-\theta_0+\frac{1}{2}\right)s_\psi,$$
$$c = \frac{h_+^2+h_\times^2}{2}\left[\left(\theta_0^2-\theta_0+\frac{1}{2}\right)c_\psi - \frac{1}{2}\right], \tag{3.48}$$

and we made use of, $\cos(2\omega_g U) = (1-t^2)/(1+t^2)$ and $\sin(2\omega_g U) = 2t/(1+t^2)$. The discriminant in equation (3.47) is then,

$$\Delta = \left(\frac{h_+^2+h_\times^2}{2}\right)^2\left[\left(\theta_0^2-\theta_0+\frac{1}{2}\right)^2 - \frac{1}{4}\right] - h_+^2h_\times^2\left(\theta_0^2-\theta_0+\frac{1}{2}\right)^2 s_\psi^2$$
$$= \left(\frac{h_+^2-h_\times^2}{2}\right)^2\left[\left(\theta_0^2-\theta_0+\frac{1}{2}\right)^2 - \frac{1}{4}\right] + h_+^2h_\times^2\left[\left(\theta_0^2-\theta_0+\frac{1}{2}\right)^2 c_\psi^2 - \frac{1}{4}\right] \tag{3.49}$$

The roots $t_\pm$ in equation (3.47) of the equation, $at^2 - 2bt + c = 0$, are real if $\Delta \geqslant 0$, from which we conclude that the inequality in equation (3.47) is satisfied:

(1) when $a > 0$ and $\Delta < 0$: the inequality in equation (3.47) is satisfied for all $U \in \mathbb{R}$;
(2) when $a > 0$ and $\Delta \geqslant 0$: the inequality in equation (3.47) is satisfied for $t = \tan(\omega_g U) < t_-$ and $\tan(\omega_g U) > t_+$;

[8] The same approximation was shown to work extremely well when we analyzed the circularly polarized case.

(3) when $a<0$ and $\Delta\geqslant 0$: the inequality in equation (3.47) is satisfied for $t_-<\tan(\omega_g U)<t_+$;
(4) when $a<0$ and $\Delta<0$: the inequality in equation (3.47) is never satisfied.

From equations (3.48) and (3.49) we then see that $a\lessgtr 0$ and $\Delta\gtrless$ imply,

$$\begin{aligned}\cos(\psi) \;&\lessgtr \frac{1}{2\theta_0(\theta_0-1)+1}\simeq\frac{1}{2\theta_0^2}\\ \cos^2(\psi)&\gtrless \frac{1}{[2\theta_0(\theta_0-1)+1]^2}-\frac{1}{4}\left(\frac{h_+}{h_\times}-\frac{h_\times}{h_+}\right)^2\left[1-\frac{1}{[2\theta_0(\theta_0-1)+1]^2}\right]\\ &\simeq \frac{1}{4\theta_0^4}-\frac{1}{4}\left(\frac{h_+}{h_\times}-\frac{h_\times}{h_+}\right)^2,\end{aligned}\tag{3.50}$$

where the last inequalities represent good approximations when $\theta_0\gg 1$. Notice that if,

$$\left|\frac{h_+}{h_\times}-\frac{h_\times}{h_+}\right|>\frac{1}{\sqrt{\theta_0(\theta_0-1)(\theta_0^2-\theta_0+1)}}\simeq\frac{1}{\theta_0(\theta_0-1)}\implies\Delta>0,\tag{3.51}$$

and options (1) and (4) are absent, and an Unruh–DeWitt detector gets excited only during parts of the period. For circularly polarized gravitational waves, $\cos(\psi)=0$, and excitations occur when,

$$t_-<\tan(\omega_g U)<t_+\,.\tag{3.52}$$

There is another important difference between detector's transition rate induced by circularly polarized and elliptically polarized gravitational waves. Upon rewriting equation (3.46) at leading order in $\mathrm{e}^{2\theta_0}$,

$$\begin{aligned}&\frac{h_+^2+h_\times^2}{2}+\left[\frac{h_+^2+h_\times^2}{2}c_\psi\cos(2\omega_g U)-\frac{h_+^2-h_\times^2}{2}s_\psi\sin(2\omega_g U)\right]\\ &\quad\times\Big[2\theta_0(\theta_0-1)+1\Big]+\mathcal{O}\left(\mathrm{e}^{-2\theta_0}\right)=4\theta_0^2\mathrm{e}^{-2\theta_0},\end{aligned}\tag{3.53}$$

we see that only the first term in equation (3.53) survives in the circularly polarized case, in which $h_+=h_\times$ and $\cos(\psi)=0$. Very close to that point, the first term $(h_+^2+h_\times^2)/2$ dominates, and the beginning of the cut is still well approximated in terms of the Lambert function as (cf equation (3.29)),

$$\theta_0(h_+,h_\times)\simeq-\Re\left[W\left(-\frac{1}{2}\sqrt{\frac{h_+^2+h_\times^2}{2}}\right)\right],\tag{3.54}$$

whose small $\bar h\equiv\sqrt{(h_+^2+h_\times^2)/2}$−expansion is highly nonanalytic. On the other hand, when deviations from the circularly polarized case are significant, the solution changes to,

$$\theta_0(h_+,h_\times)\simeq-\frac{1}{2}\ln\left[\frac{h_+^2+h_\times^2}{4}c_\psi\cos(2\omega_g U)-\frac{h_+^2-h_\times^2}{4}s_\psi\sin(2\omega_g U)\right],\tag{3.55}$$

which exists when the argument of the logarithm is positive, i.e. when $\tan(2\omega_g U)\lessgtr\left(\frac{h_+^2+h_\times^2}{h_+^2-h_\times^2}\right)\cot(\psi)$ for $(h_+^2-h_\times^2)\sin(\psi)\lessgtr 0$.

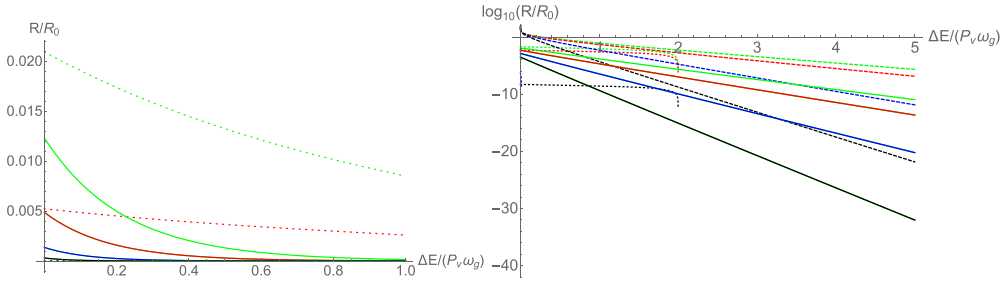

Figure 6. *Left panel:* The detector's transition rate $\mathcal{R}$ for a massless scalar as a function of $\Delta E/(P_v\omega_g)$ in units of $\mathcal{R}_0=\hbar\sqrt{\bar\gamma}P_v\omega_g/(2\pi^2)$ as measured by a freely falling Unruh–DeWitt detector. All curves are for the moment in time, $U=\pi/4\omega_g$ and for the relative phase, $\psi=\pi/2$, which is the same phase difference as for circularly polarized waves. Different curves are for different values of the gravitational strains: $h_+=0.1$ and $h_\times=0.2$ (green), $h_+=0.01$ and $h_\times=0.1$ (red), $h_+=0.01$ and $h_\times=0.001$ (blue), and $h_+=0$ and $h_\times=0.0001$ (black). *Right panel:* The same but now for $\log_{10}[\mathcal{R}/\mathcal{R}_0]$. The solid curves are numerical results, the dashed curves are obtained by using the approximation in equation (3.56), and the dotted lines correspond to the approximation in equation (3.57).

With these considerations in mind, one can obtain an approximate expression for the detector rate in the massless limit (cf equation (3.34)),

$$\mathcal{R}(U,\Delta E)\approx\frac{\hbar\sqrt{\bar\gamma}P_v\omega_g}{2\pi^2}\sqrt{\frac{P_v\omega_g}{\Delta E}}\left(\frac{h_+^2c_+^2(U)+h_\times^2c_\times^2(U)}{2}-\frac{h_+^2+h_\times^2}{4}\right)^{\frac{\Delta E}{2P_v\omega_g}}\Theta_+, \tag{3.56}$$

where $\Theta_+=1$ when the argument inside the brackets is positive (which is identical the positivity requirement on the argument of the logarithm in equation (3.55)), and $\Theta_+=0$ when it is negative. A second perturbative approximation can be obtained by expanding the integrand in equation (3.22) in powers of the gravitational strain. Making use of equation (3.42) and keeping, for simplicity, the quadratic order terms only, one obtains for the detector's transition rate in the massless scalar case,

$$\begin{aligned}\mathcal{R}(\Delta E)=\frac{\hbar\sqrt{\bar\gamma}P_v\omega_g}{2\pi}\left\{\frac{h^2(U)}{6}\left(1-\frac{\Delta E}{2P_v\omega_g}\right)^3+\frac{2h^2(U)-(h_+^2+h_\times^2)}{4}\left(1-\frac{\Delta E}{2P_v\omega_g}\right)\frac{\Delta E}{2P_v\omega_g}\right\}\\ \times\Theta(2P_v\omega_g-\Delta E)+\mathcal{O}(h_{+,\times}^4),\end{aligned} \tag{3.57}$$

where $h^2(U)=h_+^2c_+^2(U)+h_\times^2c_\times^2(U)$, and we have dropped the quartic terms as they are significantly more complicated than in the circularly polarized case in equation (3.33).

In figure 6 we show selected numerical results of integrating equation (3.43) in the massless limit, in which the transition rate reduces to (cf equation (3.31)),

$$\mathcal{R}(\Delta E)=\frac{\hbar\sqrt{\bar\gamma}P_v\omega_g}{2\pi^2}\int_{\theta_0}^\infty\frac{\mathrm{d}\theta}{\theta\left[H^2(U,\theta)-\theta^2\right]^{1/2}}\mathrm{e}^{-\frac{\Delta E}{P_v\omega_g}\theta}. \tag{3.58}$$

In the same figure, for comparison, we also show the analytical estimates from equation (3.56) (dashed) and from equation (3.57) (dotted). Notice that the latter approximation (obtained by expanding in powers of h) does not work as well as in the circularly polarized

case, as it does not need to give a positive result in the whole interval, $0 \leqslant \Delta E \leqslant 2P_v\omega_g$[9]. The detector's transition rate for a massive scalar field can be studied analogously, and therefore we leave it as an exercise.

None of the results presented in this section can be compared with those in [9], where approximations were used which do not capture the effects of the cuts in figure 1.[10]

4. Conclusions and outlook

In section 2 we generalize the massive real scalar field propagator of [1] to general gravitational waves propagating in one direction, thus relaxing the monochromatic approximation used in [1]. The Wightman two-point functions are given in equation (2.4) and the propagator in equations (2.14) and (2.15). We then show that the generalized propagator produces the one-loop results which are identical in form to the ones obtained in [1].

In section 3 we then study how a freely falling Unruh–DeWitt detector (which couples to a massless or massive scalar field) responds to the gravitational wave background. We find that the deformation of the invariant distance induced by the gravitational waves gets fully compensated by the motion of a freely falling detector[11], thus leaving the effect of the modified amplitude of vacuum fluctuations expressed by the (u,u')-dependent prefactor in equation (2.4), the effects of which we study in some detail. In this work we focus on studying detector's excitation rate induced by passing gravitational waves, i.e. the rate of transitions from the detector's ground state (with energy E_0) to an excited state E, for which $\Delta E = E - E_0 > 0$. These transitions are of a particular interest as they are completely absent in Minkowski space, and therefore—no matter how small it may be—any observed rate can be interpreted as the detection of gravitational waves.

We treat the detector's transition rate in three different approximations:

- *Numerical solution*, which can be considered to be exact. The resulting detector's excitation rate $\mathcal{R}$ is exponentially suppressed, and can be approximated by, $\mathcal{R} = \mathcal{R}_0(\Delta E, m, \omega_g)\exp\left[-\frac{\Delta E}{P_v\omega_g}\theta_0(h)\right]$, where $\theta_0(h) > 0$ is the beginning of the cut in the complex Δu plane, whose functional dependence on h is determined by equation (3.28), and it is highly nonanalytic; $\mathcal{R}_0(\Delta E, m, \omega_g)$ is a weak function of $\Delta E/(P_v\omega_g)$ and exponentially decays with increasing $m/(P_v\omega_g)$.
- Expanding in powers of h^2, where h is the gravitational wave strain. This generates a series of poles of the order $2n+2$, each of which contributes to the term $\sim h^{2n}$ when $0 \leqslant \Delta E \leqslant 2nP_v\omega_g$, the first two contributions are shown in equation (3.33) for circularly polarized gravitational waves and in equation (3.57) for general elliptically polarized gravitational waves.

  The field theoretic interpretation of these contributions is that they actively contribute when the scalar field absorbs $2\,n$ gravitons, each of which with energy $P_v\omega_g$, such that the detector's

[9] The perturbative rate can be negative if $h^2(U) < (h_+^2 + h_\times^2)/2$ and when $x_- < \Delta E/(2P_v\omega_g) < \min[x_+, 1]$, where $x_\pm$ are the roots of the equation, $x^2 + 2\left[2 - 3(h_+^2 + h_\times^2)/(2h^2(U))\right]x + 1 = 0$.

[10] Here we do not take account of the detector's rate induced by transitions to lower energy states considered in [9], for which $\Delta E < 0$, as those are absent when the detector is in its ground state, and moreover such transitions would be hard to resolve from detector's response in Minkowski vacuum. The transitions we consider excite the detector, $\Delta E > 0$, and they are completely absent in Minkowski vacuum.

[11] From equation (3.20) one sees that for timelike distances $\Delta\bar{x}^2(x;x') \to -(\Delta\tau - i\epsilon)^2$, such that in the classical limit (when $\epsilon \to 0$) $\Delta\bar{x}^2(x;x')$ reduces to the geodesic distance between points x and x', also known as the worldline. When the distance is lightlike or spacelike however, there is no classical analogue for $\Delta\bar{x}^2(x;x')$.

energy can increase by $\Delta E \leqslant 2nP_v\omega_g$. Figures 3 and 6 show that expanding in powers of the gravitational wave strain captures correctly the qualitative trend of the numerical solution, but at the quantitative level this approximation performs quite poorly.

- Expanding around the cut at $\theta = \theta_0(h)$ in equations (3.28) and (3.46) for circularly polarized and elliptically polarized gravitational waves, respectively. The leading order result is shown in equation (3.34) for circularly polarized waves and in equation (3.56) for elliptically polarized waves. This approximation captures correctly the exponential decay of the detector's excitation rate with increasing $\Delta E > 0$, that is its nonanalytic structure in the gravitational wave strain, but it fails to correctly model the exponential prefactor, as can be clearly seen from figures 3–6.

In this work we have addressed the response of an Unruh–DeWitt detector to monochromatic, unidirectional, circularly polarized and elliptically polarized, gravitational waves. A more general investigation is warranted by relaxing any of the above mentioned restrictions. It would be, in particular, of interest to calculate the transition rate of the detector induced by a stochastic gravitational wave background. But to do that properly requires knowledge of the corresponding propagator, which is presently unknown.

Data availability statement

No new data were created or analysed in this study.

Appendix A. Derivation of the Wightman functions

Here we briefly present a derivation of the Wightman functions by the method of mode sums. Upon expanding the scalar field operator in terms of the momentum space mode functions $\phi_\pm(u,\vec{k})$ and the creation and annihilation operators $\hat{a}^\dagger(\vec{k})$ and $\hat{a}(\vec{k})$,

$$\hat{\phi}(u,\vec{x}_\perp,v) = \int \frac{\mathrm{d}^{D-2}k_\perp \mathrm{d}k^{D-1}}{(2\pi)^{D-1}} \mathrm{e}^{i\vec{k}_\perp\cdot\vec{x}_\perp} \Big[\mathrm{e}^{-\frac{i}{2}\Omega_-(\vec{k})v}\phi_+(u,\vec{k})\hat{a}(\vec{k}) + \mathrm{e}^{\frac{i}{2}\Omega_+(\vec{k})v}\phi_-(u,\vec{k})\hat{a}^\dagger(-\vec{k})\Big], \tag{A.1}$$

which obey a standard non-vanishing commutation relation,

$$\Big[\hat{a}(\vec{k}),\hat{a}^\dagger(\vec{k}')\Big] = (2\pi)^{D-1}\delta^{D-1}(\vec{k}-\vec{k}'),$$

one obtains the following expressions for the positive and negative frequency Wightman functions,

$$i\Delta^{(+)}(x;x') = \langle\Omega|\,\hat{\phi}(x)\hat{\phi}(x')\,|\Omega\rangle = \int \frac{\mathrm{d}^{D-1}k}{(2\pi)^{D-1}}\,\mathrm{e}^{i\vec{k}_\perp\cdot\Delta\vec{x}_\perp - \frac{i}{2}\Omega_-(\vec{k})\Delta v}\phi_+(u,\vec{k})\phi_-(u',-\vec{k}), \tag{A.2}$$

$$\begin{aligned} i\Delta^{(-)}(x;x') &= \langle\Omega|\,\hat{\phi}(x')\hat{\phi}(x)\,|\Omega\rangle = \int \frac{\mathrm{d}^{D-1}k}{(2\pi)^{D-1}}\,\mathrm{e}^{i\vec{k}_\perp\cdot\Delta\vec{x}_\perp + \frac{i}{2}\Omega_+(\vec{k})\Delta v}\phi_-(u,\vec{k})\phi_+(u',-\vec{k}) \\ &= \int \frac{\mathrm{d}^{D-1}k}{(2\pi)^{D-1}}\,\mathrm{e}^{-i\vec{k}_\perp\cdot\Delta\vec{x}_\perp + \frac{i}{2}\Omega_-(\vec{k})\Delta v}\phi_-(u,-\vec{k})\phi_+(u',\vec{k}), \end{aligned} \tag{A.3}$$

where $\Delta\vec{x}_\perp = \vec{x}_\perp - \vec{x}'_\perp$, $\Delta v = v - v'$, and we have assumed,

$$\hat{a}(\vec{k})|\Omega\rangle = 0, \qquad (\forall\vec{k}\in\mathbb{R}^{D-1}). \tag{A.4}$$

The functions $\phi_+(u,\vec{k})$ and $\phi_-(u',\vec{k})$ are the positive and negative frequency mode functions obeying,

$$\left(\partial_u \pm \frac{i}{2\Omega_\mp}\left[\left(g^{ij}(u)-\delta^{ij}_\perp\right)k_ik_j\right]\pm\frac{i}{2}\Omega_\pm\right)\left[\gamma^{1/4}(u)\phi_\pm(u,\vec{k})\right]=0, \tag{A.5}$$

where $\Omega_\pm(\vec{k})=\omega\pm k^{D-1}$, $\gamma(u)=\det[g_{ij}(u)]$, and $\omega=\sqrt{\|\vec{k}\|^2+m^2}$. This is a first order differential equation in u and therefore can be easily solved. The properly normalized, ground state solutions of equation (A.5) are given by,

$$\phi_\pm(u,\vec{k})=\frac{1}{\gamma^{1/4}(u)}\sqrt{\frac{\hbar}{2\omega}}\exp\left[\mp\frac{i\Omega_\pm}{2}\left(u+\frac{k_ik_j}{\omega_\perp^2}\int^u \mathrm{d}\bar{u}\left(g^{ij}(\bar{u})-\delta^{ij}\right)\right)\right], \tag{A.6}$$

where $\omega_\perp^2=\omega^2-(k^{D-1})^2$ and $\omega^2=\|\vec{k}\|^2+m^2$. The factor $\gamma^{-1/4}(u)$ in the normalization of the mode functions (A.6) can be traced back to the Wronskian condition for the mode functions (which in turn originates from canonical quantization). Together with the condition (A.4), the choice of pure positive (negative) frequency solutions for the functions ϕ_+ (ϕ_-) in equation (A.1) uniquely specify the Gaussian state of the system, which we consider the vacuum state. More general (pure) Gaussian states can be obtained by exacting a Bogolyubov transformation on the operators $\hat{a}(\vec{k})$ and $\hat{a}^\dagger(\vec{k})$. However, these states are excited states of the system, in the sense that their energy per mode is higher than the energy of the state $|\Omega\rangle$ defined in equation (A.4). In that respect the state $|\Omega\rangle$ used here to quantize the scalar field and calculate the Wightman functions can be considered as the vacuum state.

Upon inserting the mode functions (A.6) into equation (A.2) and converting $\mathrm{d}k^{D-1}$ into $\mathrm{d}\Omega_+$ one obtains,

$$\begin{aligned} i\Delta^{(+)}(x;x') &= \frac{\hbar}{[\gamma(u)\gamma(u')]^{1/4}}\int\frac{\mathrm{d}^{D-2}k_\perp}{2(2\pi)^{D-1}}\mathrm{e}^{i\vec{k}_\perp\cdot\Delta\vec{x}_\perp}\int_0^\infty\frac{\mathrm{d}\Omega_+}{\Omega_+}\\ &\quad\times\exp\left\{-\frac{i}{2}\left[\Omega_+\left(1+\frac{(\mathcal{G}^{xx}(u;u')-1)k_x^2+(\mathcal{G}^{yy}(u;u')-1)k_y^2+2\mathcal{G}^{xy}(u;u')k_xk_y}{\omega_\perp^2}\right)\right.\right.\\ &\quad\left.\left.\times\Delta u+\frac{\omega_\perp^2}{\Omega_+}\Delta v\right]\right\}, \end{aligned} \tag{A.7}$$

where

$$\mathcal{G}^{ij}(u;u')=\frac{1}{\Delta u}\int_{u'}^u g^{ij}(\bar{u})\,\mathrm{d}\bar{u},\qquad(\Delta u=u-u'). \tag{A.8}$$

One can evaluate the Ω_+-integral in equation (A.7) by making use of equation (3.471.9) in [20],

$$\begin{aligned} i\Delta^{(+)}(x;x') &= \frac{\hbar}{[\gamma(u)\gamma(u')]^{1/4}}\int\frac{\mathrm{d}^{D-2}k_\perp}{(2\pi)^{D-1}}\mathrm{e}^{i\vec{k}_\perp\cdot\Delta\vec{x}_\perp}K_0\\ &\quad\times\left(\omega_\perp\sqrt{-\Delta u_\epsilon\Delta v_\epsilon\left(1+\frac{\mathcal{G}^{xx}k_x^2+\mathcal{G}^{yy}k_y^2+2\mathcal{G}^{xy}k_xk_y}{\omega_\perp^2}\right)}\right), \end{aligned} \tag{A.9}$$

where we have introduced a shorthand notation for the $i\epsilon$ prescriptions, $\Delta u_\epsilon\equiv\Delta u-i\epsilon$ and $\Delta v_\epsilon\equiv\Delta v-i\epsilon$. The argument squared of the modified Bessel function of the second kind K_0 is a quadratic form $Q(k_x,k_y)$ which can be diagonalized by a simple $\mathcal{G}^{ij}$-dependent rotation. For that purpose the eigenvalues and determinant of $\mathcal{G}^{ij}$ are useful,

$$\mathcal{G}_\pm=\frac{1}{2}\left(\mathcal{G}^{xx}+\mathcal{G}^{yy}\right)\pm\sqrt{\frac{1}{4}\left(\mathcal{G}^{xx}-\mathcal{G}^{yy}\right)-\left(\mathcal{G}^{xy}\right)^2} \tag{A.10}$$

$$\mathcal{G}^{-1}(u;u') \equiv \det\left[\mathcal{G}^{ij}\right] = \mathcal{G}_+\mathcal{G}_- = \mathcal{G}^{xx}\mathcal{G}^{yy} - (\mathcal{G}^{xy})^2\,. \tag{A.11}$$

Upon rotating the momenta (k_x,k_y) into the diagonal frame $(\tilde{k}_x,\tilde{k}_y)$ and renormalizing them as, $(\bar{k}_x,\bar{k}_y) = (\sqrt{\mathcal{G}_+}\tilde{k}_x, \sqrt{\mathcal{G}_-}\tilde{k}_y)$, equation (A.9) reduces to,

$$i\Delta^{(+)}(x;x') = \frac{1}{[\gamma(u)\gamma(u')]^{1/4}\sqrt{\det[\mathcal{G}^{ij}]}}\int\frac{\mathrm{d}^{D-2}\bar{k}_\perp}{(2\pi)^{D-1}}\mathrm{e}^{i\vec{\bar{k}}_\perp\cdot\Delta\vec{\bar{x}}_\perp}K_0\Big(\bar{\omega}_\perp\sqrt{-\Delta u_\epsilon\Delta v_\epsilon}\Big), \tag{A.12}$$

where $\bar{\omega}_\perp^2 = \bar{k}_x^2+\bar{k}_y^2+\sum_{n=3}^{D-2}k_n^2+m^2$ (the sum contributes when $D>4$) and $\Delta\vec{\bar{x}}$ is defined by, $\vec{\bar{k}}_\perp\cdot\Delta\vec{\bar{x}} = \vec{\bar{k}}_\perp\cdot\Delta\vec{\bar{x}}$. By expressing $\mathrm{d}^{D-2}k$ in spherical coordinates and integrating over the angles, equation (A.12) can be recast as,

$$\begin{aligned} i\Delta^{(+)}(x;x') = {}& \frac{\hbar}{[\gamma(u)\gamma(u')]^{1/4}\sqrt{\det[\mathcal{G}^{ij}]}}\frac{1}{\|\Delta\vec{\bar{x}}_\perp\|^{\frac{D-4}{2}}} \\ & \times\int_0^\infty\frac{\mathrm{d}\bar{k}_\perp}{(2\pi)^{\frac{D}{2}}}\bar{k}_\perp^{\frac{D-2}{2}}J_{\frac{D-4}{2}}\left(\bar{k}_\perp\|\Delta\vec{\bar{x}}_\perp\|\right)K_0\left(\bar{\omega}_\perp\sqrt{-\Delta u_\epsilon\Delta v_\epsilon}\right), \end{aligned} \tag{A.13}$$

The final integral over $\bar{k}_\perp$ can be evaluated by using (6.596.7) in [20],

$$\begin{aligned} i\Delta^{(+)}(x;x') = {}& \frac{\hbar m^{D-2}}{(2\pi)^{D/2}[\gamma(u)\gamma(u')]^{1/4}\sqrt{\det[\mathcal{G}^{ij}](u;u')}} \\ & \times\frac{K_{\frac{D-2}{2}}\left(m\sqrt{-(\Delta u-i\epsilon)(\Delta-i\epsilon)+\|\Delta\vec{\bar{x}}_\perp\|^2}\right)}{\left(m\sqrt{-(\Delta u-i\epsilon)(\Delta v-i\epsilon)+\|\Delta\vec{\bar{x}}_\perp\|^2}\right)^{\frac{D-2}{2}}}, \end{aligned} \tag{A.14}$$

where we have restored the original $i\epsilon$ prescriptions and where,

$$\|\Delta\vec{\bar{x}}_\perp\|^2 = \sum_{i,j=1,2}\Delta x^i\mathcal{G}_{ij}(u;u')\Delta x^j + \sum_{n=3}^{D-2}\Delta x_n^2, \tag{A.15}$$

where the sum contributes when $D>4$. $\mathcal{G}_{ij}(u;u')$ is the matrix inverse of $\mathcal{G}^{ij}(u;u')$, $\mathcal{G}^{ik}(u;u')\mathcal{G}_{kj}(u;u') = \delta^i_{\ j}$, such that:

$$\mathcal{G}(u;u') \equiv \det[\mathcal{G}_{ij}(u;u')] = \frac{1}{\det[\mathcal{G}^{ij}]}\,. \tag{A.16}$$

The negative frequency Wightman function (A.3) satisfies, $i\Delta^{(-)}(x';x) = i\Delta^{(+)}(x;x')$ and

$$i\Delta^{(-)}(x;x') = \left[i\Delta^{(+)}(x;x')\right]^*, \tag{A.17}$$

and therefore $i\Delta^{(-)}(x;x')$ can be obtained by taking a complex conjugate of equation (A.14), reproducing the Wightman functions in equation (2.4).

Appendix B. Inverse quartic root cuts

In the case of polarized gravitational waves, the cut structure in the complex plane may be richer than the one shown in figure 1. To see that, let us analyse the term $1/[\gamma(u)\gamma(u')]^{1/4}$ in equation (3.22) in the complex Δu-plane. For simplicity we consider here maximally polarized

gravitational waves. Let us begin with the + polarization. Recalling that $u = U + \Delta u/2$ and $u' = U - \Delta u/2$ one can write,

$$\gamma(u) = 1 - h_+^2 \cos^2(\omega_g u) = 1 - \frac{h_+^2}{2}\big[1 + \cos(2\omega_g U)\cos(\omega_g \Delta u) - \sin(2\omega_g U)\sin(\omega_g \Delta u)\big],$$

from which we infer,

$$\begin{aligned}\gamma(u)\gamma(u') = 1 - h_+^2\big[1 + \cos(2\omega_g U)\cos(\omega_g \Delta u)\big] \\ + \frac{h_+^4}{4}\big[(1 + \cos(2\omega_g U)\cos(\omega_g \Delta u))^2 - \sin^2(2\omega_g U)\sin^2(\omega_g \Delta u)\big].\end{aligned}$$

To see that there are poles in the complex Δu plane, let us transform this equation into the variables, $\omega_g \Delta u \to 2i\theta - 2\zeta$,

$$\begin{aligned}\cosh^2(2\theta + 2i\zeta) - 2\left(\frac{2}{h_+^2} - 1\right)\cos(2\omega_g U)\cosh(2\theta + 2i\zeta) \\ + \left(\frac{4}{h_+^4} - \frac{4}{h_+^2} + \cos(2\omega_g U)\right) = 0.\end{aligned} \tag{B.1}$$

The roots of this quadratic equation are given by,

$$[\cosh(2\theta + 2i\zeta)]_\pm = \left(\frac{2}{h_+^2} - 1\right)\cos(2\omega_g U) \pm i\frac{2}{h_+}\sqrt{\frac{1}{h_+^2} - 1}\sin(2\omega_g U), \tag{B.2}$$

or equivalently,

$$\begin{aligned}\cosh(2\theta) = \frac{2}{h_+^2} - 1 \implies \theta_\pm = \frac{1}{2}\ln\left[\frac{2}{h_+^2} - 1 \pm \frac{2}{h_+}\sqrt{\frac{1}{h_+^2} - 1}\right] \\ = \pm\frac{1}{2}\ln\left[\frac{2}{h_+^2} - 1 + \frac{2}{h_+}\sqrt{\frac{1}{h_+^2} - 1}\right], (\zeta_\pm)_n = \pm\omega_g U + \pi n, (n \in \mathbb{Z}).\end{aligned} \tag{B.3}$$

The poles in the case of $\times$-polarized gravitational waves are given by simply replacing $h_+ \to h_\times$. The result in equation (B.3) shows that singly polarized gravitational waves generate a richer structure of cuts in the complex Δu plane. In particular, the term $1/[\gamma(u)\gamma(u')]^{1/4}$ generates four of its own inverse quartic root cuts (for $n = 0$), whose real parts 'walk' along the real axis as, $\Re[\Delta u] = \pm\, 2U$, and the cuts begin at, $\Im[\Delta u] = \theta_\pm/\omega_g$. In this work we not attempt to model the detector's excitation rate due to these cuts.

ORCID iD

Tomislav Prokopec https://orcid.org/0000-0003-0391-5743

References

[1] van Haasteren R and Prokopec T 2022 Scalar propagator for planar gravitational waves (arXiv:2204.12930 [gr-qc])
[2] Garriga J and Verdaguer E 1991 Scattering of quantum particles by gravitational plane waves *Phys. Rev.* D **43** 391–401
[3] Jones P, McDougall P and Singleton D 2017 Particle production in a gravitational wave background *Phys. Rev.* D **95** 065010
[4] Jones P, McDougall P, Ragsdale M and Singleton D 2018 Scalar field vacuum expectation value induced by gravitational wave background *Phys. Lett.* B **781** 621–5

[5] Zhang P M, Duval C, Gibbons G W and Horvathy P A 2017 The memory effect for plane gravitational waves *Phys. Lett.* B **772** 743–6
[6] Zhang P M, Duval C, Gibbons G W and Horvathy P A 2018 Velocity memory effect for polarized gravitational waves *J. Cosmol. Astropart. Phys.* JCA05(2018)030
[7] Siddhartha M and Dasgupta A 2020 Scalar and fermion field interactions with a gravitational wave *Class. Quantum Grav.* **37** 105001
[8] Xu Q, Ahmad S A and Smith A R H 2020 Gravitational waves affect vacuum entanglement *Phys. Rev.* D **102** 065019
[9] Chen B H and Chiou D W 2022 Response of the Unruh–DeWitt detector in a gravitational wave background *Phys. Rev.* D **105** 024053
[10] Unruh W G 1976 Notes on black hole evaporation *Phys. Rev.* D **14** 870
[11] DeWitt B S, Hawking S W and Israel W 1979 *General Relativity: an Einstein Centenary Survey* (Cambridge: Cambridge University Press)
[12] Birrell N D and Davies P C W 2012 *Quantum Fields in Curved Space* (Cambridge: Cambridge University Press)
[13] Bourgoin A, Poncin-Lafitte C L, Mathis S and Angonin M C, Impact of dipolar magnetic fields on gravitational wave strain by galactic binaries (arXiv:2201.03226 [gr-qc])
[14] Amaro-Seoane P *et al* Astrophysics with the laser interferometer space antenna (arXiv:2203.06016 [gr-qc])
[15] Gibbons G W 1975 Quantized fields propagating in plane wave space-times *Commun. Math. Phys.* **45** 191–202
[16] Louko J and Satz A 2008 Transition rate of the Unruh–DeWitt detector in curved spacetime *Class. Quantum Grav.* **25** 055012
[17] Louko J and Satz A 2006 How often does the Unruh–DeWitt detector click? Regularisation by a spatial profile *Class. Quant. Grav.* **23** 6321–44
[18] Bose S, Mazumdar A, Morley G W, Ulbricht H, Toroš M, Paternostro M, Geraci A, Barker P, Kim M S and Milburn G 2017 Spin entanglement witness for quantum gravity *Phys. Rev. Lett.* **119** 240401
[19] Marshman R J, Mazumdar A and Bose S 2020 Locality and entanglement in table-top testing of the quantum nature of linearized gravity *Phys. Rev.* A **101** 052110
[20] Gradshteyn I S and Ryzhik I M 2014 *Table of Integrals, Series and Products* (New York: Academic)